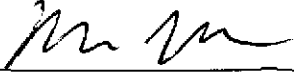

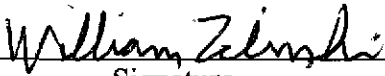
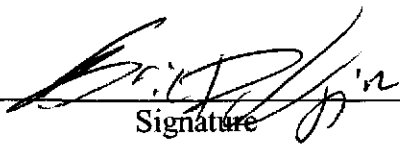

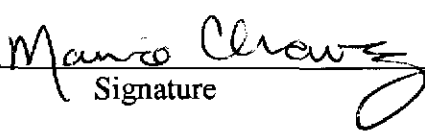


539437

Sandia National Laboratories
Waste Isolation Pilot Plant

**Analysis Report for BRAGFLO
Preliminary Modeling Results With New Gas Generation Rates
Based Upon Recent Experimental Results**

Author:	Martin Nemer (6821)		4-19-05
	Print	Signature	Date
Author:	Josh Stein (6821)		4-19-2005
	Print	Signature	Date
Author:	William Zelinski (6821)		4-19-05
	Print	Signature	Date
Technical Review:	Eric Vugrin (6821)		4/20/05
	Print	Signature	Date
Management Review:	David Kessel (6821)		4/20/05
	Print	Signature	Date
QA Review:	Mario Chavez (6820)		4/19/05
	Print	Signature	Date

WIPP: 1.4.1.1: PA: QA-L: PKg 539377

Information Only

Table of Contents

1	Executive Summary.....	4
2	Introduction and Objectives.....	4
3	Approach	5
4	Methodology.....	5
4.1	Updating Microbial Degradation Rates.....	6
4.1.1	Microbial Degradation Rates used in the CCA, 1997 PAVT, 2004 CRA PA	6
4.1.2	Determination of Updated Degradation Rates	10
4.2	Implementation in BRAGFLO.....	17
4.2.1	Accounting for Early Gas Generation at a High Rate.....	18
4.2.2	Accounting for Additional Uncertainties in Microbial Viability.....	19
5	Results OF BRAGFLO Simulations.....	21
5.1	Pressure	21
5.2	Brine Saturation	26
5.3	Brine Outflow	31
6	Run Control	37
6.1.1	Explanation of Run Control Tables	45
7	References	46
	Appendix A	48
	Appendix B	55
	Appendix C.....	57

List of Figures

Figure 1.	Carbon dioxide produced in experiments that were inundated, inoculated, amended, and with excess nitrate.	7
Figure 2.	Carbon dioxide produced in experiments that were inundated, inoculated, unamended, without excess nitrate.....	8
Figure 3.	Carbon dioxide produced in humid experiment.....	9
Figure 4.	Least-squares fit of the data in Figure 1.....	12
Figure 5.	Least-squares fit of the data in Figure 2.....	13
Figure 6.	Least-squares fit of the data in Figure 3.....	14
Figure 7.	Least-squares fit of the inundated, amended samples.	15
Figure 8.	Scatter plot of pressure in the waste panel for scenario S1.	22
Figure 9.	Scatter plot of pressure in the waste panel for scenario S2.....	23
Figure 10.	Pressure in the waste panel versus time for scenario S1	24
Figure 11.	Pressure in the waste panel versus time for scenario S2.....	25
Figure 12.	Scatter plot of brine saturation in the waste panel for scenario S1.	27
Figure 13.	Scatter plot of brine saturation in the waste panel for scenario S2.....	28
Figure 14.	Brine saturation in the waste panel versus time for scenario S1.....	29
Figure 15.	Brine saturation in the waste panel versus time for scenario S2.....	30
Figure 16.	Scatter plot of cumulative brine outflow in the waste panel for scenario S1	32
Figure 17.	Scatter plot of cumulative brine outflow in the waste panel for scenario S2.....	33
Figure 18.	Pressure, cumulative brine inflow and outflow in the waste panel versus time for vector 22 in scenario S1	34
Figure 19.	Cumulative brine outflow in the waste panel versus time for scenario S1.....	35
Figure 20.	Cumulative brine outflow in the waste panel versus time for scenario S2.....	36
Figure 21.	Cumulative brine flow up the bore hole to the Culebra formation.....	37

List of Tables

Table 1. Relevant least-squares results for microbial gas-generation rates.....	16
Table 2. Rates converted for use in BRAGFLO.....	17
Table 3. Times of points plotted.....	21
Table 4. BRAGFLO Run Control Files: Step 1.....	38
Table 5. BRAGFLO Run Control Files: Step 2.....	40
Table 6. BRAGFLO Run Control Files: Step 3.....	41
Table 7. BRAGFLO Run Control Files: Step 4.....	42
Table 8. BRAGFLO Run Control Files: Step 3, Exception Runs	43
Table 9. BRAGFLO Run Control Files: Step 4, Exception Runs	44
Table 10. Amount of CO ₂ accumulated versus time for the inundated, inoculated, amended, and with excess nitrate experiment.....	49
Table 11. Least-Squares slopes and intercepts from the data in Table 10.....	50
Table 12. Analysis of variance for the data in Table 10 and Table 11.....	50
Table 13. Amount of carbon dioxide versus time produced in experiments that were inundated, inoculated, unamended, without excess nitrate	51
Table 14. Least-Squares slopes and intercepts <i>S</i> from the data in Table 13.....	51
Table 15. Analysis of variance for the data in Table 13 and Table 14.....	51
Table 16. Amount of carbon dioxide produced versus time in humid experiment.....	52
Table 17. Least-Squares slopes and intercepts from the data in Table 16.....	52
Table 18. Analysis of variance for the data in Table 16 and Table 17.....	52
Table 19. Amount of carbon dioxide produced versus time for the inundated, amended, no excess nitrate experiment	53
Table 20. Least-Squares slopes and intercepts from the data in Table 19.....	54
Table 21. Analysis of variance for the data in Table 19 and Table 20.....	54
Table 22. Values of x_a in equation (10) for determining the 95% confidence interval using the student's t distribution ...	54
Table 23. Cellulosics inventory from the 2004 CRA PA.....	55
Table 24. Conversion of the masses of cellulose, plastics, and rubber into equivalent amounts of cellulose.....	55

1 EXECUTIVE SUMMARY

Microbial gas-generation rates for the consumption of cellulose, plastic, and rubber (CPR) materials in the WIPP were determined from 10 years of experimental data gathered at Brookhaven National Laboratory. Rates used in the CCA, the 1997 PAVT, and the 2004 CRA PA were obtained from the first three years of the BNL experiment. Compared to the CCA, 1997 PAVT, and 2004 CRA PA, the rate of microbial gas generation decreases significantly over the 10-year period. Using the proposed gas-generation rates from the entire 10 year BNL data, BRAGFLO was run to determine the impact of the lower long-term gas-generation rates. The BRAGFLO results indicate lower average pressures and higher brine saturation, and a lower rate of pressurization of the repository. The impact that these results could have on total releases has not been determined in the present analysis. However, the results of this analysis do not suggest that total releases will be significantly affected.

2 INTRODUCTION AND OBJECTIVES

In 1996, the U.S. Department of Energy (DOE) completed a performance assessment (PA) for the Waste Isolation Pilot Plant (WIPP). The PA was part of the Compliance Certification Application (CCA) submitted to the Environmental Protection Agency (EPA) to demonstrate compliance with the long-term radioactive disposal standards of 40 CFR 191 (subparts B and C) (U.S. EPA, 1993) and the associated certification criteria of 40 CFR 194 (U.S. EPA, 1996). Based on the CCA and subsequent information and analyses, the EPA certified the WIPP's compliance in May 1998. As required by the WIPP Land Withdrawal Act (Public Law 102-579 [as amended by Public Law 104-201]) (U. S. Congress, 1992), DOE is required to submit documentation of continued compliance to EPA for the recertification of the WIPP every five years following the first receipt of waste.

The purpose of this analysis is to provide an evaluation of proposed changes to WIPP PA that incorporate new specific and general information concerning the probability and rate of microbial gas generation in the repository after closure. This analysis was conducted according to the Analysis Plan AP-116 (Stein and Nemer, 2005) and is a programmatic decision. The changes under consideration partly reflect concerns that the EPA expressed during a technical exchange in Dallas in January 2005. The exchange was associated with the EPA review of the first Compliance Recertification Application (CRA) submitted by the DOE in March 2004 (U.S. DOE, 2004). The EPA's concerns were focused on the probability of microbial gas generation. Advances in microbiology have found microbes existing in a wide variety of so called "extreme" environments that were previously considered devoid of life. With this information, the EPA argued that the probability of significant microbial activity and concomitant microbial gas generation occurring in the WIPP should be changed from 0.5 to 1, which results in either 50% or 100% of the realizations having microbial activity. The DOE responded that there is a significant probability that microbial activity would slow considerably as microbes use the available electron acceptors and the geochemical environment in the waste rooms changed with time. This expectation has been confirmed by gas-generation experiments performed at Brookhaven National Laboratory (BNL). Microbial gas-generation rates in the CCA, the 1997 Performance Assessment Verification Test (PAVT) and the CRA-2004 Performance Assessment (2004 CRA PA) were based upon the first 1 to 3 years of data from these experiments, but approximately 10 years of data are now available. The extended range of data shows much slower rates of gas generation after the first few years. During

the January 2005 technical exchange, DOE agreed to consider the idea of a probability of 1 for microbial activity but favored the use of gas-generation rates in the WIPP PA models that reflect the longer-term experimental results, the use of electron acceptors, and expected changes in the environment of the waste-storage areas. In this preliminary study all realizations have microbial activity. To account for uncertainty in the probability of attaining the BNL microbial-gas-generation rates, DOE has used a sampled-multiplicative factor applied to the rates with a uniform distribution between 0 and 1.

3 APPROACH

The primary purpose of this analysis, referred to in this document as the new-rate analysis, was to assess the potential impact of proposed changes to microbial gas generation on BRAGFLO modeling results. Changing the microbial gas-generation rates also involved raising the initial pressure to account for the increased gas-generation rate in the first few years of the experiments, but this is considered to be an integral part of the adjustment in microbial gas-generation rates. Microbial gas generation also occurs in 100% of the vectors in this analysis versus 50% in the CCA, the 1997 PAVT and the 2004 CRA PA. This analysis does not implement the removal of methanogenesis from WIPP PA, which was evaluated independently (Nemer and Zelinski, 2005).

The methodology for implementing these changes is also being tested prior to making any permanent changes in the BRAGFLO modeling process and the WIPP Parameter Database. This work was conducted in accordance with Analysis Plan AP-116, written specifically to guide revision of the microbial gas-generation modeling process (Stein and Nemer, 2005). Results for the first 3 years of gas-generation experiments by BNL (Francis et al., 1997) were the basis for microbial gas-generation rates used in the CCA, the 1997 PAVT and the 2004 CRA PA. This analysis updates the microbial gas-generation rates used in BRAGFLO with results that reflect the entire 10 years of experimental data.

In this preliminary analysis, no changes were made to the WIPP Parameter Database. Instead, all changes were implemented through manual modification of input control files at different stages of the BRAGFLO modeling process (Long, 2004). The output variables of interest are pressure, saturation, and brine flow, as they affect subsequent compliance-modeling analyses. Brine saturation and pressure are inputs to the calculation of Direct Brine Release (DBR) and Spallings releases. Brine outflow is an input to the calculation of flow and transport through the Salado Formation and the Culebra Member of the Rustler Formation.

Two scenarios were calculated: the undisturbed scenario (S1), and a disturbed scenario (S2), which models a drilling penetration through the waste panel into a pressurized brine pocket in the Castile Formation at 350 years. Scenario S2 produced the highest brine outflows in previous analyses. These two scenarios bound the full range of results in all six scenarios that constitute the full suite of BRAGFLO analyses required for a complete PA calculation.

4 METHODOLOGY

This analysis was separated into two separate but related tasks: calculation of new zeroth-order microbial gas-generation rates based on long-term BNL experimental data, and implementation of the new rates and associated uncertainties in BRAGFLO to test the impact of these changes on repository behavior.

4.1 *Updating Microbial Degradation Rates*

Microbial gas-generation rates used in the CCA, the 1997 PAVT, and 2004 CRA PA were based on three years of BNL experimental data. The first task of this analysis was to analyze the full 10 years of experimental data to develop updated distributions of the microbial gas-generation rates.

The microbial gas-generation rate parameters used by BRAGFLO are WAS_AREA: GRATMICI and WAS_AREA: GRATMICH. The parameter GRATMICI is the rate of microbial gas generation from consumption of CPR materials in a brine-inundated environment, and GRATMICH is the humid gas-generation rate. The microbial inoculum was prepared from a mixture of WIPP-relevant samples in accordance with procedures described by Francis et. al., 1997. Conversion of the rates from experimental conditions to WIPP conditions is described below in §4.1.2.

4.1.1 *Microbial Degradation Rates used in the CCA, 1997 PAVT, 2004 CRA PA*

The BNL experimental data, used to define the gas-generation rates, are plotted in Figure 1- Figure 3. Diamond points in were available at the time of the CCA. Square points were available later. Each figure includes a line, which defines the rate developed from the early data available at the time of the CCA. Note that the same figures appear in AP-116, however the figure captions in AP-116 have several mistakes. The figure captions below are correct.

Figure 1 is a plot of CO₂ generation as a function of time for inundated experiments that were anaerobic, inoculated, and given excess nutrients and nitrate. The maximum inundated rate developed for the CCA was defined as the slope of the line determined by two data points at 69 and 411 days (Wang and Brush, 1996a).

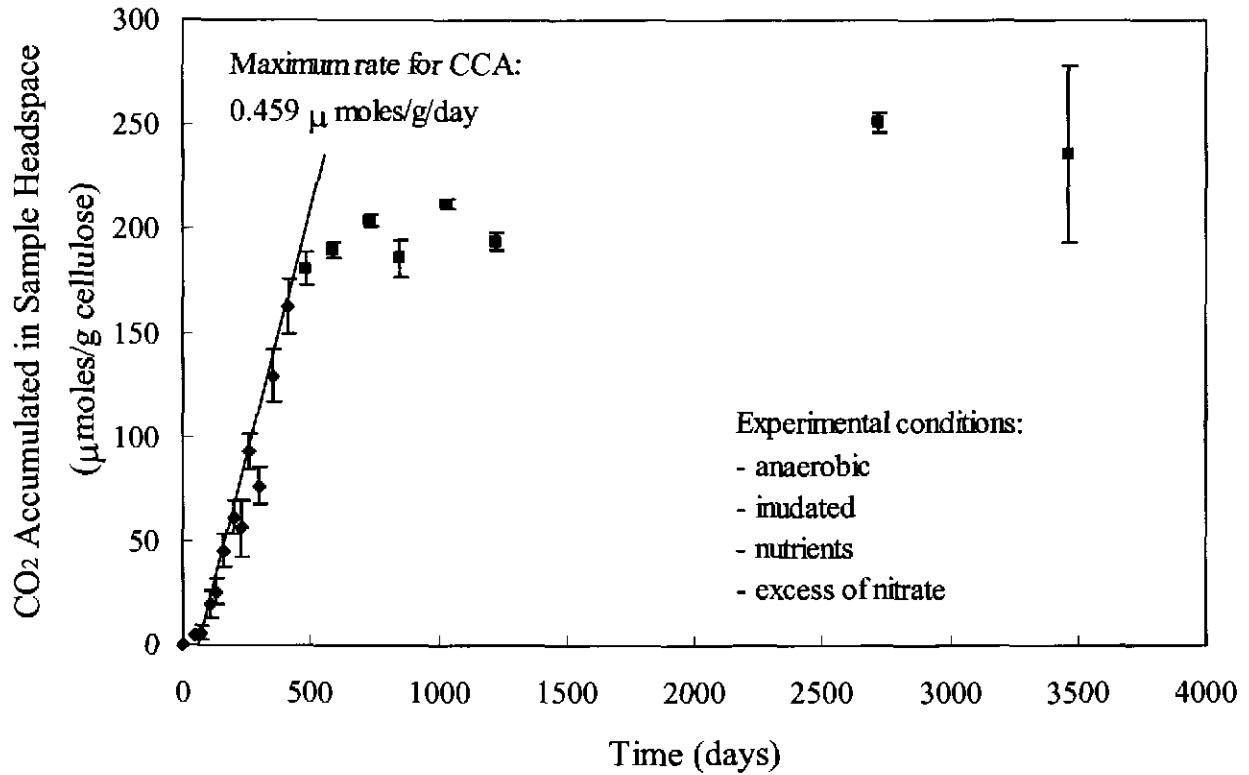


Figure 1. Carbon dioxide produced in experiments that were inundated, inoculated, amended, and with excess nitrate (Francis et al., 1997; U. S. DOE, 2002). Diamond points were available at the time of the CCA. Square points in were available later. The slope of line represents the initial gas-generation rate used in CCA, the 1997 PAVT and the 2004 CRA PA. Points represent the mean of triplicate samples. Error bars represent the standard error. The raw data for this plot is listed in Table 10, in Appendix A.

Figure 2 is a plot of CO₂ generation as a function of time for inundated experiments that were anaerobic, inoculated with microbes but unamended with nutrients. These experiments were used to define the minimum inundated rate. The minimum inundated rate developed for the CCA is shown as a line, defined as the slope of the line determined by two data points at 0 and 1034 days (Wang and Brush, 1996a).

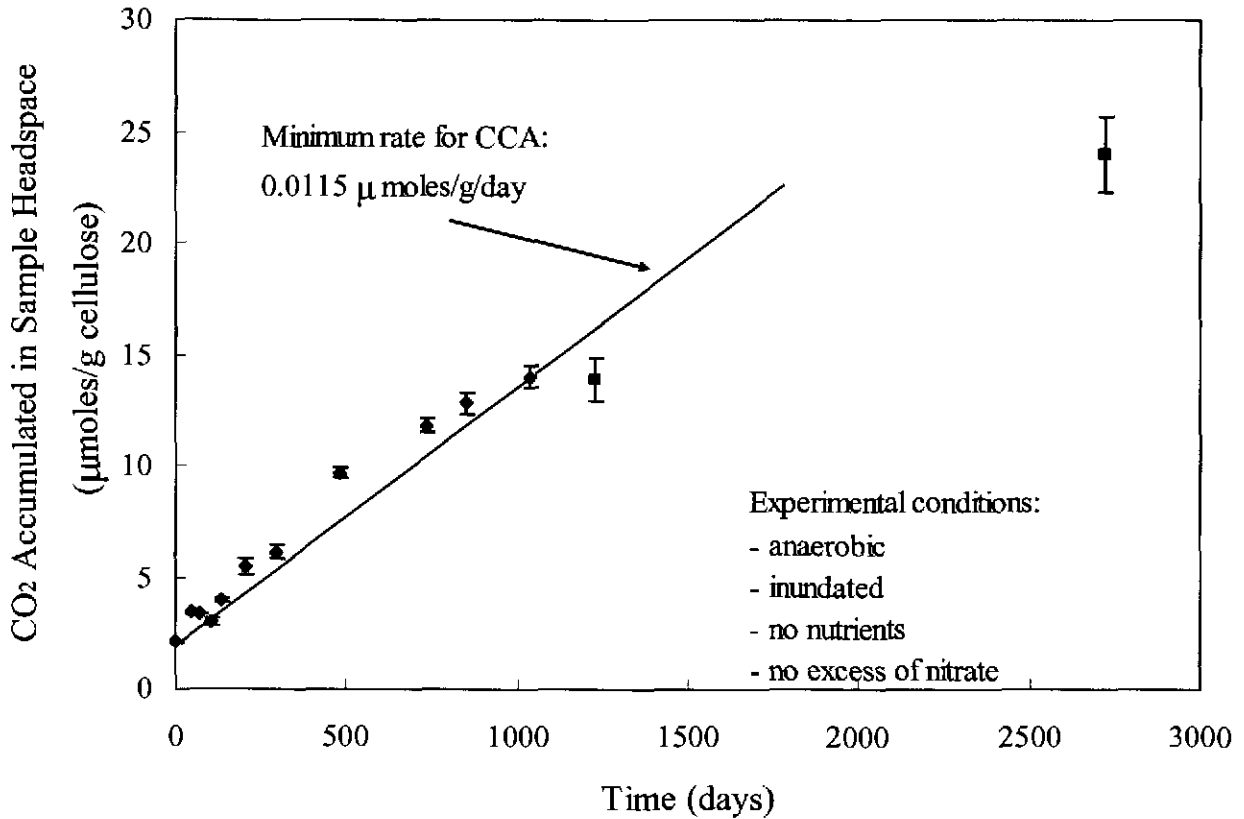


Figure 2. Carbon dioxide produced in experiments that were inundated, inoculated, unamended, without excess nitrate (Francis et al., 1997; U. S. DOE, 2002). Points, error bars, and lines are the same as Figure 1. The raw data in this plot is listed in Table 13, in Appendix A.

Figure 3 is a plot of CO₂ generation as a function of time for humid experiments that were anaerobic, inoculated, and unamended with nutrients. These experiments were used to define the maximum humid rate. The minimum humid rate was taken to be zero in the CCA, the 1997 PAVT, and the 2004 CRA PA. As in previous figures, the maximum humid rate developed during the CCA is shown as a line, defined as the slope of the line determined by two data points at 6 and 415 days (Wang and Brush, 1996a).

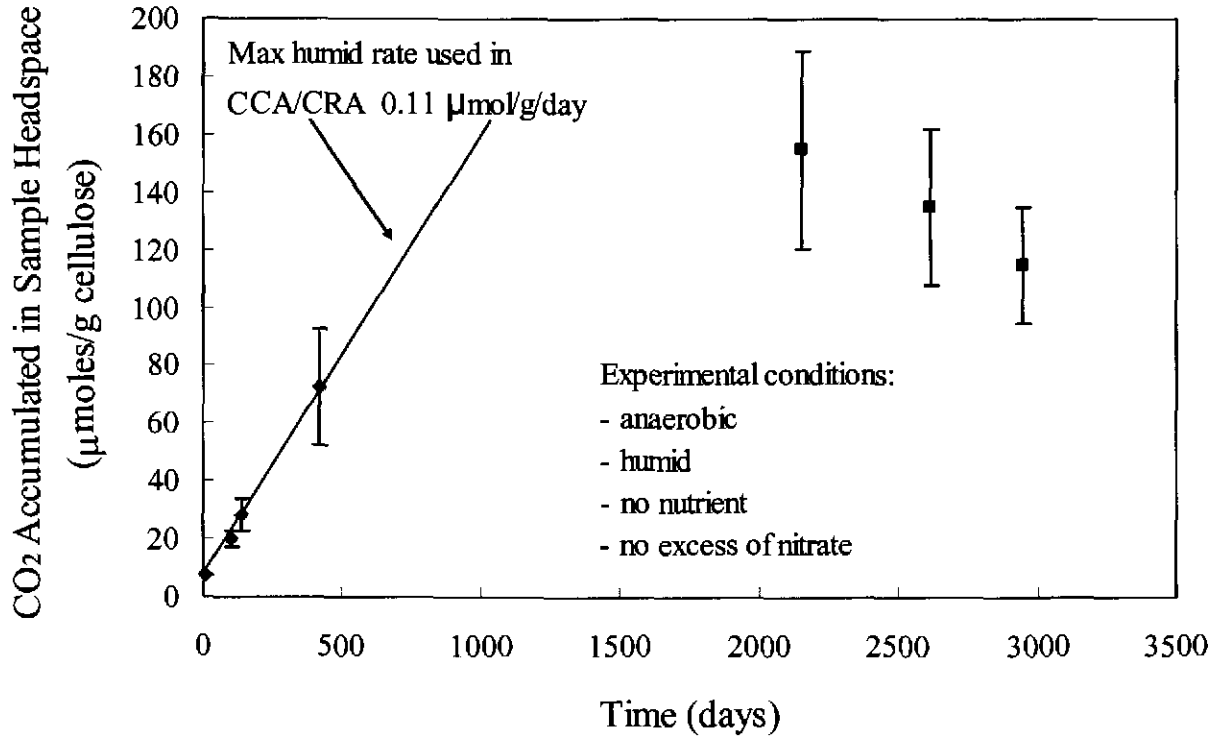


Figure 3. Carbon dioxide produced in humid experiment (Francis et al., 1997; U. S. DOE, 2002). Points, error bars, and lines are the same as Figure 1. The raw data for this plot is listed in Table 16, in Appendix A.

The complete 10 year BNL data shown in Figure 1-Figure 3 indicates an initial rapid period of gas generation followed by a slower long-term period. While it is not precisely known why the rate of microbial activity decreased in the BNL experiments, a decrease in the rate of microbial activity is commonly observed in many systems. The decreased rate of microbial activity is attributed to sequential use of different electron acceptors, different substrates, and the build-up of microbial metabolites (Monod, 1949). In geochemical systems, microbes sequentially use electron acceptors that yield decreasing amounts of free energy ΔG (Froelich et al., 1979; Berner, 1980; Criddle et al., 1991; Chapelle, 1993; Wang and Van Cappellen, 1996; Schlesinger, 1997; Hunter et al., 1998; Fenchel et al., 2000). The order of use of electron acceptors is: oxygen, nitrate, manganese (IV)oxides, iron (III) oxides, sulfate, followed by CO₂ (methanogenesis). Microbes also use the available substrates sequentially in order of decreasing biodegradability; from amorphous to crystalline cellulose. Additionally, increasing concentrations of microbial byproducts such as CO₂ will eventually limit or inhibit microbial activity.

4.1.2 Determination of Updated Degradation Rates

To accommodate both the rapid-short-term and slower long-term behavior of the experimentally determined microbial gas-generation in BRAGFLO, the complete-10-year-gas-generation data were modeled using two linear functions, corresponding to a short-term rate and a long-term rate. The rate was assumed to switch from the short-term rate to the long-term rate at an experimental data point. To solve for the short-term and long-term rates, a least squares fit of the mean data was constructed in which the residual S between the observed and fitted values of accumulated CO_2 is

$$S(m) = \sum_{i=1}^m (y_i - a_s - b_s t_i)^2 + \sum_{i=m}^n (y_i - a_l - b_l t_i)^2, \quad (1)$$

where a_s, b_s are the short-term intercept and slope, a_l, b_l are the long-term intercept and slope, m is index of the data point where the fit changes from the short-term to the long-term rate, n is the number of data points, y_i is the mean amount of gas produced up to time t_i , and i is the index running from 1 to n . The slopes and intercepts as a function of m are given by (Box et al., 1978)

$$b_s(m) = \frac{m \sum_{i=1}^m t_i y_i - \sum_{i=1}^m t_i \sum_{i=1}^m y_i}{m \sum_{i=1}^m t_i^2 - \left(\sum_{i=1}^m t_i \right)^2}, \quad a_s(m) = \frac{\sum_{i=1}^m t_i^2 \sum_{i=1}^m y_i - \sum_{i=1}^m y_i \sum_{i=1}^m t_i y_i}{m \sum_{i=1}^m t_i^2 - \left(\sum_{i=1}^m t_i \right)^2}, \quad (2)$$

$$b_l(m) = \frac{(n-m+1) \sum_{i=m}^n t_i y_i - \sum_{i=m}^n t_i \sum_{i=m}^n y_i}{(n-m+1) \sum_{i=m}^n t_i^2 - \left(\sum_{i=m}^n t_i \right)^2}, \quad a_l(m) = \frac{\sum_{i=m}^n t_i^2 \sum_{i=m}^n y_i - \sum_{i=m}^n y_i \sum_{i=m}^n t_i y_i}{(n-m+1) \sum_{i=m}^n t_i^2 - \left(\sum_{i=m}^n t_i \right)^2}, \quad (3)$$

where m ranged from 3 to $n-2$ such that neither the short-term or long-term fits were determined from less than three data points. Given the fits as a function of the integer m , m was then selected to minimize the residual sum of squares S . Given that the mean and the standard errors in the data based on triplicate samples were reported (Francis et al., 1997; U. S. DOE, 2002), it can be shown (Ginevan, 2004) that using the mean values to determine the fit and the variance in the fit parameters is statistically representative of the underlying data. Thus the variance in the long-term slope b_l was determined by,

$$V(b_l) = \frac{s^2}{\sum (\bar{t} - t_i)^2}, \quad (4)$$

where

$$\bar{t} = \frac{1}{n-m+1} \sum t_i, \quad (5)$$

and s is the sample standard deviation,

$$s^2 = \frac{S_l(m)}{(n-m+1)-2}. \quad (6)$$

In equation (6) the minus 2 comes from the two parameters in the fit (the slope and the intercept). The long-term portion of the residual sum of squares, $S_l(m)$, is given by the second term in equation (1),

$$S_l(m) = \sum_{i=m}^n (y_i - a_l - b_l t_i)^2. \quad (7)$$

The standard deviation in the slope is then given by

$$\sigma(b_l) = \sqrt{V(b_l)}. \quad (8)$$

A confidence interval on the slope was determined using the student's t distribution. In this statistical method we look for a value x_α such that the probability of a random variable x (having a student's t distribution with $n-m-1$ degrees of freedom) attaining a value greater in magnitude than x_α is equal to the desired probability level α

$$P(|x| > x_\alpha) = \alpha, \quad (9)$$

where P is the probability determined from the student's t distribution with $n-m-1$ degrees of freedom. Here we have chosen $\alpha = 0.05$ which corresponds to the 95% confidence interval. The standard deviation in equation (8) is then multiplied by x_α to give the endpoints of the 95% confidence interval on the long-term slope,

$$\text{confidence interval} = b_l \pm x_\alpha \sigma. \quad (10)$$

Because only the long-term slope is used in BRAGFLO, we did not calculate the variances in the intercepts a_s , a_l or the short-term slope b_s . A least-squares fit was generated for each set of data corresponding to Figure 1-Figure 3. The results of this fitting procedure are shown below in Figure 4-Figure 6. Additionally data from an inundated-nutrient-amended experiment were fitted and is shown in Figure 7. The detailed calculations using the above formulas are given in Appendix A. Note that only the first two digits of the below calculations are significant since generally only two

digits were given in the experimental data; however we have calculated to 6 digits to avoid round off errors.

To obtain the most information out of a PA analysis it is important to use the maximum available uncertainty while maintaining physical realism. Thus in obtaining our maximum and minimum microbial-gas-generation rates for BRAGFLO we took the maximum and minimum endpoints of the 95% confidence intervals (see equations (10)-(11)) of the three fits of the three experiments given in Figure 4, Figure 5, and Figure 7. The data in Figure 7 were not used in the CCA, the PAVT and the 2004 CRA PA because the short-term rate determined at that time (from the first three years of data) is greater than the short-term rate obtained from the unamended data shown in Figure 2. Looking over the entire 10 year period, the long-term mean rates from the two experiments are indistinguishable. However over the 10-year period the lower endpoint of the 95% confidence interval for the inundated-and-amended experiment, shown in Figure 7, is lower than the corresponding endpoint of the unamended experiment shown in Figure 5. Thus we believe the data and fit shown in Figure 7 should be used to determine the minimum rate and this rate was used in BRAGFLO for this analysis. The observation that the mean rates in Figure 5 and Figure 7 are indistinguishable at long-times suggests that the effect of initially adding nutrients to the sample dissipates at sufficiently long times.

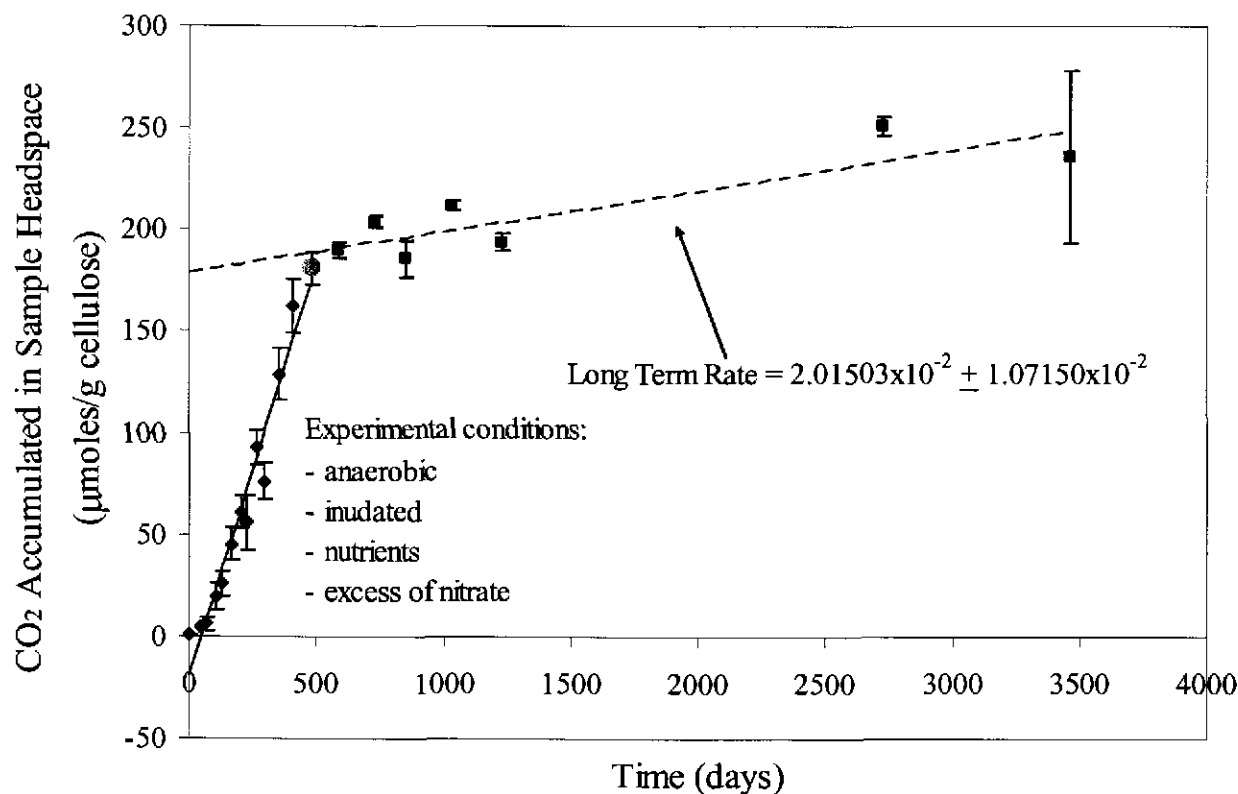


Figure 4. Least-squares fit of the data in Figure 1. Lines correspond to the least-squares fits. Diamond points and the solid line correspond to the short-term data set, square points and the dashed line correspond to the long-term data set. The circle point corresponds to the point *m* where the rate switches from its short-term to its long-term value. The point *m* is common to both the short- and long-term fits. Points represent the mean of triplicate samples. Error bars represent the standard error.

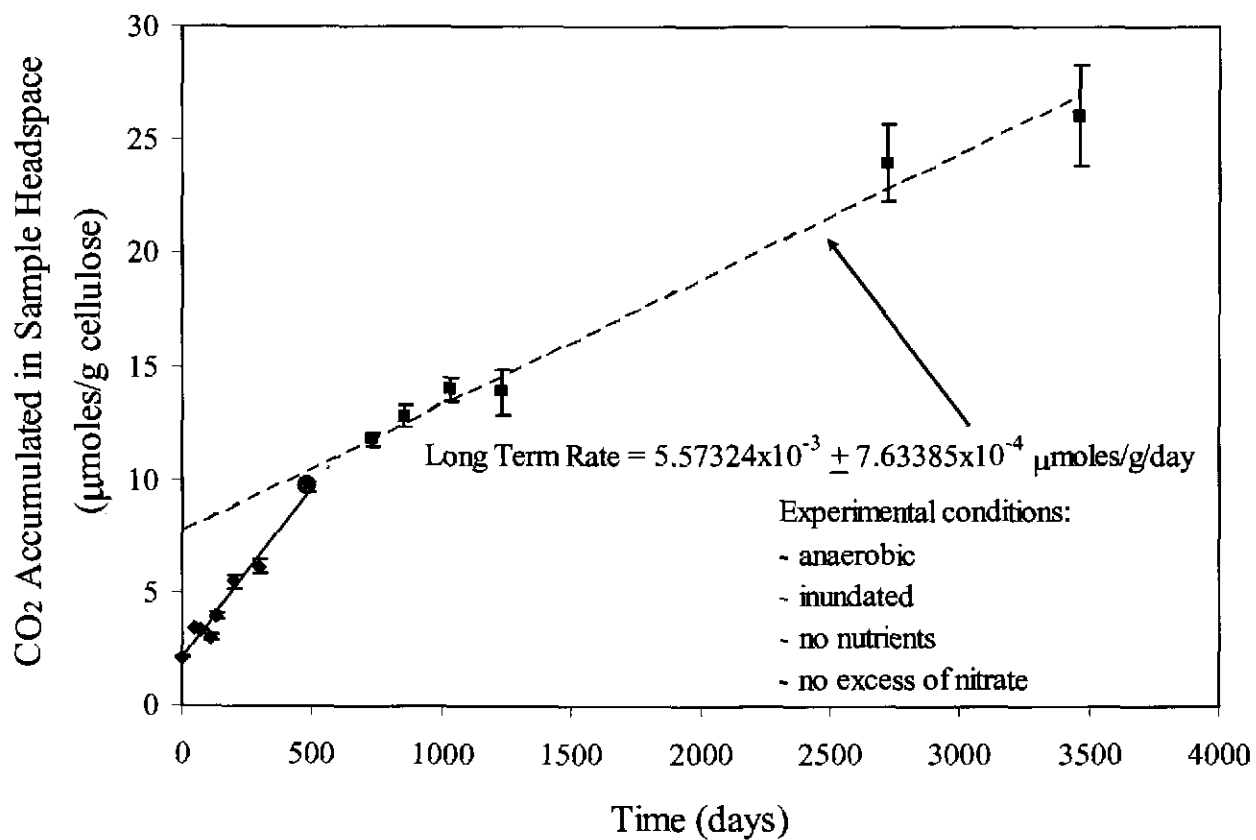


Figure 5. Least-squares fit of the data in Figure 2. Points, error bars, and lines are the same as in Figure 4.

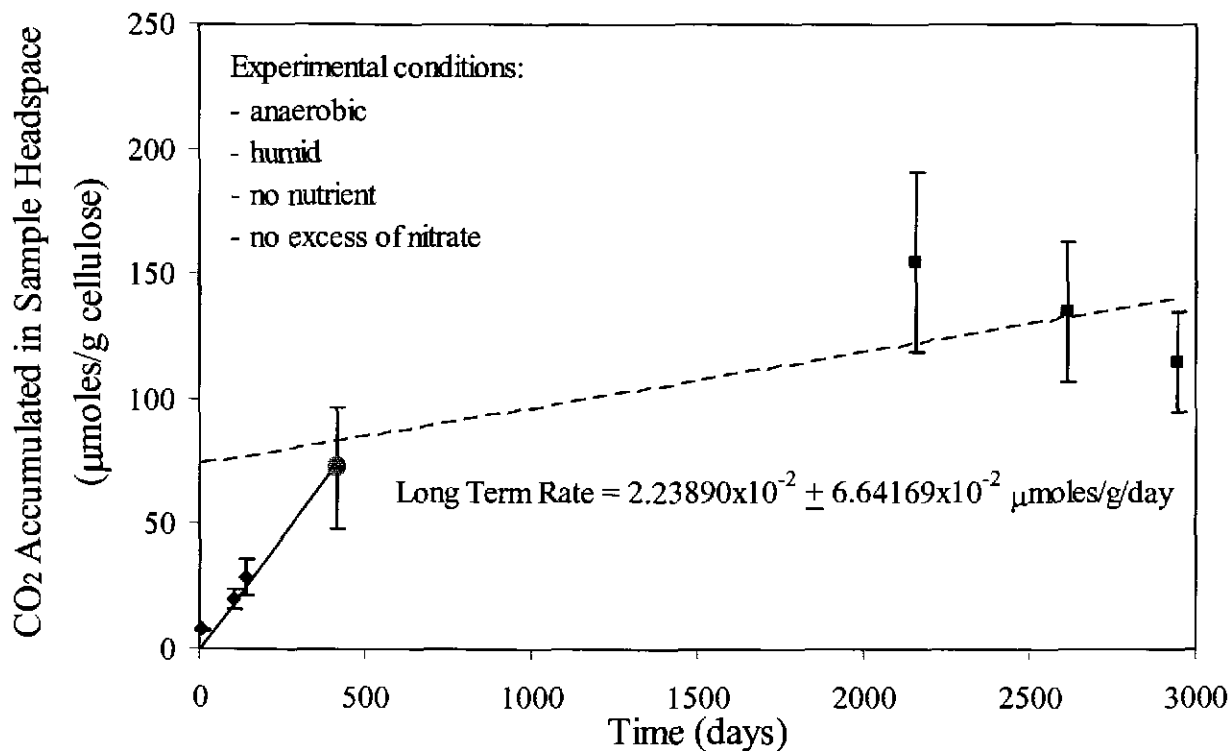


Figure 6. Least-squares fit of the data in Figure 3. Points, error bars, and lines are the same as in Figure 4.

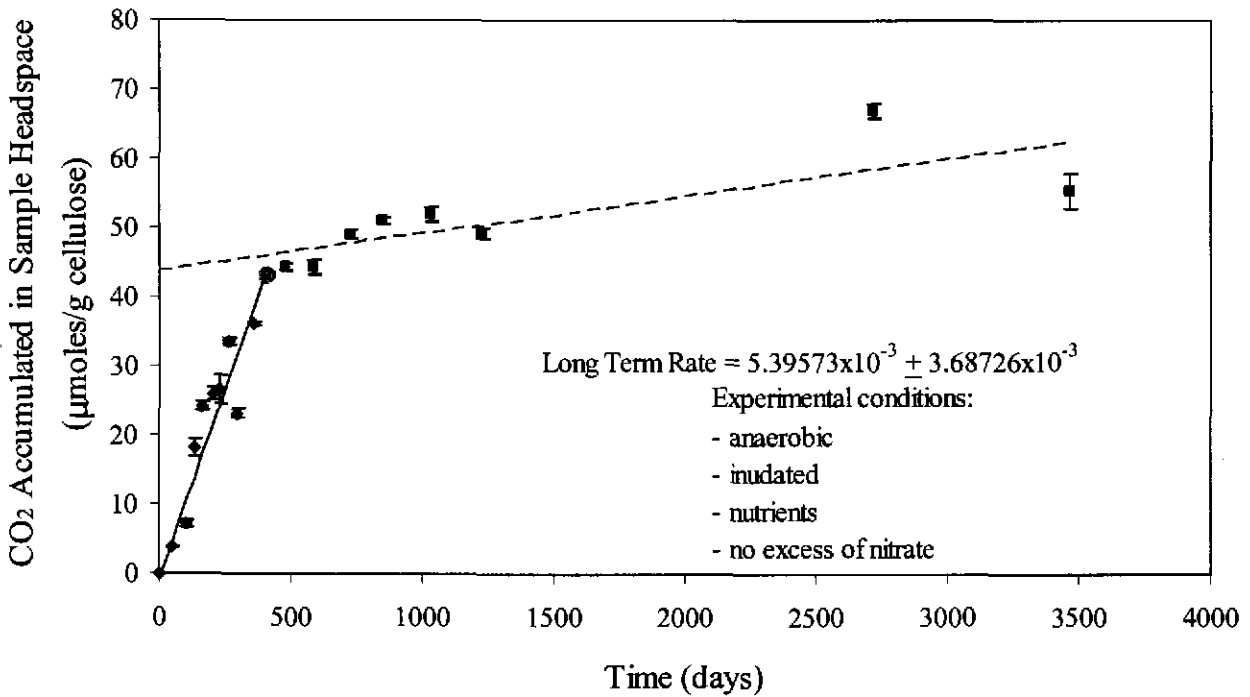


Figure 7. Least-squares fit of the inundated, amended samples (Francis et al., 1997; U. S. DOE, 2002). These data were not used in the CCA, the 1997 PAVT, or the 2004 CRA PA. However, the minimum long-term rate ($0.00171 = 0.0054 - 0.0037$) is less than that given by the data in Figure 5. Here the points, error bars, and lines have the same meaning as in Figure 4. The raw data for this figure is listed in Table 19, in Appendix A.

Table 1 lists the relevant least-squares results from Figure 4, Figure 6 and Figure 7; also listed are the slopes of the lines in Figure 1-Figure 3, which were to determine the gas-generation rates used in the CCA, the 1997 PAVT, and the 2004 CRA PA. The time and amount of gas produced up to the point m are also listed. In the fourth column of Table 1, the maximum and minimum rates are taken to be the endpoints of the 95% confidence interval,

$$\begin{aligned} \text{max rate} &= b_l + x_\alpha \sigma, \\ \text{min rate} &= b_l - x_\alpha \sigma. \end{aligned} \quad (11)$$

Table 1. Relevant least-squares results for microbial gas-generation rates. In column four, the maximum rate was obtained by adding $x_\alpha \sigma$, and the minimum rate was obtained by subtracting $x_\alpha \sigma$, as given by equation (11).

		b_s ($\mu\text{mol/g/day}$)	$b_l \pm x_\alpha \sigma$ ($\mu\text{mol/g/day}$)	time at m (days)	gas at m ($\mu\text{mol/g}$)
CCA, 1997 PAVT, 2004 CRA PA maximum inundated rate	Figure 1	0.459	-	-	-
CCA, 1997 PAVT, 2004 CRA PA minimum inundated rate	Figure 2	0.0115	-	-	-
CCA, 1997 PAVT, 2004 CRA PA maximum humid rate	Figure 3	0.11	-	-	-
proposed maximum inundated rate	Figure 4	-	3.08653×10^{-2}	481	181
proposed minimum inundated rate	Figure 7	-	1.70847×10^{-3}	411	43.2
proposed maximum humid rate	Figure 6	-	8.88060×10^{-2}	415	72.6

BRAGFLO uses gas-generation rates in units of moles carbon/kg cellulose/sec, whereas the BNL experiments measured the accumulation of CO_2 in units of $\mu\text{mol CO}_2$ /gram cellulose. The conversion to BRAGFLO units is given by,

$$\begin{aligned} \text{rate} \left(\frac{\text{mol C}}{\text{kg cell year}} \right) &= \text{rate} \left(\frac{\mu\text{mol CO}_{2(g)}}{\text{g cell day}} \right) \times 365 \frac{\text{days}}{\text{year}} \times 1000 \frac{\text{g}}{\text{kg}} \times 10^{-6} \frac{\text{mol}}{\mu\text{mol}} \times 1.56 \frac{\text{mol CO}_2}{\text{mol CO}_{2(g)}} \times 1 \frac{\text{mol C}}{\text{mol CO}_2}, \quad (12) \\ \text{rate} \left(\frac{\text{mol C}}{\text{kg cell sec}} \right) &= \text{rate} \left(\frac{\text{mol C}}{\text{kg cell year}} \right) \times \frac{1 \text{ year}}{31556930 \text{ sec}}. \end{aligned}$$

Here a 1.56 correction factor for the amount of CO_2 dissolved in the brine (Wang and Brush, 1996a) has been applied to the inundated rate but not the humid rate. This correction factor is related to the partition coefficient of CO_2 between the gas phase and the brine phase. Because the experimental CO_2 measurements were made in the gas phase, they need to be corrected to account for the amount of CO_2 dissolved into the brine phase. The converted rates are given in Table 2.

The results in Table 2 indicate that the proposed maximum long-term humid rate is greater than the proposed maximum long-term inundated rate. A possible explanation of the overlap is that the humid experimental conditions may have overlapped with the inundated conditions. In particular, the humid samples may have been at least partially inundated with brine during the experiment. To reconcile this discrepancy, in BRAGFLO calculations the sampled humid rate was constrained to be less than or equal to the sampled inundated rate. The BRAGFLO implementation of this decision is explained in §4.2. As in the CCA, 1997 PAVT, 2004 CRA PA the proposed minimum humid rate is taken to be zero.

Table 2. Rates converted for use in BRAGFLO.

	CCA, 1997 PAVT, 2004 CRA PA (mol C/kg/year)	proposed rates (mol C/kg/year)	BRAGFLO Input proposed rates (mol C/kg/sec)
Max inundated rate	0.300	0.0175747	5.56921×10^{-10}
Min inundated rate	0.010	0.000972803	3.08269×10^{-11}
max humid rate	0.040	0.0324142	1.02717×10^{-9}

4.2 Implementation in BRAGFLO

The second task of the analysis plan was to implement the proposed microbial-gas-generation rates in BRAGFLO. The BRAGFLO code is limited to a single zeroth-order reaction rate that is a function of the “effective” brine saturation in each waste cell. The effective brine saturation is calculated as the sum of the predicted brine saturation and a wicking factor (WAS_AREA:SAT_WICK), which is sampled randomly from a uniform distribution between 0 and 1; the sum is of the two is constrained to be less than or equal to 1. The rate of microbial gas generation, q_{rgm} , used in BRAGFLO is given by:

$$q_{rgm} = (R_{mi}S_{b,eff} + R_{mh}S_g^*)D_c y M_{H_2}, \quad (13)$$

where

- R_{mi} = inundated microbial degradation rate [mol C consumed / kg CPR /s],
- R_{mh} = humid microbial degradation rate [mol C consumed / kg CPR /s],
- $S_{b,eff}$ = effective brine saturation,
- S_g^* = $(1-S_{b,eff})$ if $S_{b,eff} > 0$,
= 0 if $S_{b,eff} = 0$,
- M_{H_2} = molecular weight of H_2 [kg/mol],
- D_c = initial mass concentration of CPR in the repository [kg/m³],
- y = average stoichiometric factor for microbial degradation of cellulose [moles of H_2 generated per mole C consumed].

Here one mole of cellulose ($C_6H_{10}O_5$) contains 6 mol of C (organic carbon).

The rates, R_{mi} and R_{mh} , were sampled from a uniform distribution whose range was determined in §4.1.2. For this preliminary analysis the rates were not changed in the parameter database. Rather they were altered by manually changing the sampling range in the PRELHS output transfer file, which is the LHS input file. The following lines show the relevant section of the input file in the 2004 CRA PA and in the analysis presented here:

2004 CRA PA

UNIFORM	WAS_AREA	GRATMICI
	3.17100E-10	9.51290E-09
UNIFORM	WAS_AREA	GRATMICH
	0.00000E+00	1.26840E-09

Proposed rates using data in Table 2:

UNIFORM	WAS_AREA	GRATMICI
	3.08269E-11	5.56921E-10
UNIFORM	WAS_AREA	GRATMICH
	0.00000E+00	1.02717E-9

The name and class of the PRELHS output file are given in §6. The sampled humid rate was further constrained to always be less than or equal to the sampled inundated rate,

$$R_{mh} = \min(R_{mi}, R_{mh}). \quad (14)$$

This was implemented in the ALGEBRA input file run before PREBRAG using the following line:

GRATMICH = MIN(GRATMICH,GRATMICI).

The name and class of the ALGEBRA input file are given in §6.

4.2.1 Accounting for Early Gas Generation at a High Rate

In the current formulation, the gas generation rate used by BRAGFLO only changes as a function of brine saturation and not time. Because the gas-generation rates were derived from long-term data, it was necessary to account for the gas generated in the short-term period of time during which the short-term rates apply. The total amount of gas generated in the repository during the period of faster rates was taken from the amount of gas produced in the inundated, amended + nitrate experiment (Figure 4) up to the point where the rate changes from the short-term rate to the long-term rate. From Table 1 this time corresponds to 481 days, at which 181 $\mu\text{mol/g}$ cellulose were produced. Conversion of this amount of gas to repository conditions was accomplished by

$$M_{gas} = 181 \times 10^{-6} \frac{\text{mol CO}_{2(g)}}{\text{g cell}} \times 1.56 \frac{\text{mol CO}_2}{\text{mol CO}_{2(g)}} \times \frac{1 \text{ mol cell}}{6 \text{ mol CO}_2} \times \left(\frac{162 \text{ g cell}}{\text{mol cell}} \right) \times \frac{1 \text{ mol gas}}{2 \text{ mol C}} \times 1.069 \times 10^9 \text{ mol C} = 4.07667 \times 10^6 \text{ mol C}, \quad (15)$$

where the molecular weight of cellulose is 162 g/mol, and the inventory of CPR in the repository is $1.06947 \times 10^9 \text{ mol C}$, as calculated in Appendix B. The factor of one half comes from the microbial-gas-generation conceptual model (Wang and Brush, 1996b) which at most produces half a mol of gas per mol of organic carbon when all CO_2 is sequestered by MgO. The moles of gas, M_{gas} , was converted to a pressure using the ideal equation of state at room temperature $T = 293 \text{ K}$,

$$p = \frac{M_{gas} RT}{V} = 26.714 \text{ KPa}, \quad (16)$$

where $R = 8.31451 \text{ kg m}^2/(\text{mol sec K})$ is the ideal-gas constant, and $V = 371768.4 \text{ m}^3$ is the effective volume of the repository calculated from

$$V=(\text{REFCON:VREPOS})*(\text{WAS_AREA:POROSITY}). \quad (17)$$

Here REFCON:VREPOS is the excavated storage volume of the repository and WAS_AREA:POROSITY is the effective porosity of the waste-filled repository; both REFCON:VREPOS and WAS_AREA:POROSITY are elements of the parameter database. To accommodate this pressure in BRAGFLO, the additional 26.714 KPa was assumed to be generated instantaneously upon closure of the repository. Upon closure the pressure in the waste area WAS_AREA and the rest-of-repository REPOSIT was set to

$$P_{\text{initial}} = 101,325 + 26,714 = 128,039 \text{ KPa}. \quad (18)$$

This was implemented by altering the MATSET input file with the addition of the following two lines to the end of the file:

```
PROPERTY_VALUES, MAT=CAVITY_1, NAME*VALUE: PRESSURE = 1.28039e+005
PROPERTY_VALUES, MAT=CAVITY_2, NAME*VALUE: PRESSURE = 1.28039e+005
```

The MATSET input file name and class are given in §6.

4.2.2 Accounting for Additional Uncertainties in Microbial Viability

The EPA has suggested that the probability of microbial gas generation in the WIPP should be increased to 1, from the present value of 0.5. This was implemented in BRAGFLO by changing the distribution of the sampled input parameter, WAS_AREA: PROBDEG. The probability of only cellulose being consumed was changed to 0.75, and the probability of all CPR materials being available for consumption was maintained at 0.25. These changes were implemented by manually editing the PRELHS transfer file, the input file to LHS:

2004 CRA PA

USER DISTRIBUTION	(DELTA)	WAS_AREA PROBDEG
3	SPECIFIED	DISCRETE
0.00000E+00	0.50000	
1.00000E+00	0.25000	
2.00000E+00	0.25000	

Proposed scheme

USER DISTRIBUTION	(DELTA)	WAS_AREA PROBDEG
3	SPECIFIED	DISCRETE
0.00000E+00	0.00000E+00	
1.00000E+00	0.75000	
2.00000E+00	0.25000	

The PRELHS output file name and class are given in §6.

The conditions inside the WIPP are likely to be quite different from the conditions represented in the experiments, which were designed to promote microbial growth. In the WIPP the following uncertainties may cause microbial action to be reduced from that observed in the experiments (Brush, 2004):

1. Whether microbes will survive for a significant fraction of the 10,000-year regulatory period
2. Whether sufficient H₂O will be present
3. Whether sufficient quantities of biodegradable substrates will be present
4. Whether sufficient electron acceptors will be present and available
5. Whether enough nutrients will be present and available Reference?

Due to these and other uncertainties an additional sampled parameter was added to these calculations. This additional parameter is a multiplicative factor in determining the effective microbial-gas-generation rates. For this analysis, a parameter BIOGENFC was created with a uniform distribution from 0 to 1. A uniform distribution was chosen to reflect the fact that we have no quantitative data on the effect of items 1-6 above on the probability of attaining the BNL gas generation rates. BIOGENFC was manually added to the MATSET output file as a property of the material, WAS_AREA (Block 18). This is required so that the POSTLHS modeling step can use the parameter. BIOGENFC and its distribution (uniform from 0 to 1) were also manually substituted for place-holder parameter #11 in the PRELHS output file:

2004 CRA PA

UNIFORM	REFCON	LHSBLANK
0.00000E+00	1.00000E+00	

Proposed scheme

UNIFORM	WAS_AREA	BIOGENFC
0.00000E+00	1.00000E+00	

The PRELHS output file name and class are given in §6. The calculation of gas generation rate was modified in the ALGEBRA modeling step by multiplying the gas generation rate by BIOGENFC in the ALGEBRA input file:

2004 CRA PA

KBGSI = GRATMICI*CONCBIO

KBGSH = GRATMICH*CONCBIO

Proposed scheme

KBGSI = GRATMICI*CONCBIO*BIOGENFC

$$\text{KBGSH} = \text{GRATMICH} * \text{CONCBIO} * \text{BIOGENFC}$$

Here KBGSI, and KBGSH are the inundated and humid microbial-gas-generation rates used by BRAGFLO. The ALGEBRA input file name and class are given in §6.

5 RESULTS OF BRAGFLO SIMULATIONS

Two significant changes were made to BRAGFLO simulations in this analysis. 1) Microbial gas generation rates were adjusted according to experimental results. 2) All vectors now have microbial gas generation versus 50% in the 2004 CRA PA. Increasing the probability of microbial degradation to 100% tended to increase pressure and decrease brine saturation in the waste areas, but decreasing the microbial gas generation rates tended to decrease pressure and increase brine saturation.

Scatter and time plots in Figure 8-Figure 20 compare results from calculations from this analysis and those of the 2004 CRA PA. The time intervals for points in both sets of plots are listed in Table 3.

Table 3. Times of points plotted.

Period (years)	Points plotted every (years)
0-500 years	10
500-1000 years	20
1000-10000	100

Scatter plots for both scenarios show point pairs for the entire 10,000-year modeling period. Significant differences from the 2004 CRA PA will be indicated by the distance of points from the diagonal line. Plots of high, low and average values are also compared over the entire modeling period to evaluate the effects of the change on overall modeling results. These lines do not represent individual vectors but rather the statistics for all vectors as a function of time.

5.1 Pressure

Pressure is an input parameter from BRAGFLO into the DBR and Spallings analyses. Pressure has to exceed the hydrostatic pressure (about 8 MPa) for there to be any release in a drilling-disturbance scenario.

Figure 8 and Figure 9 are scatter plots of pressure in the repository for scenarios, S1 and S2, respectively. The points above the diagonal line (higher pressure in the new-rate analysis) represent vectors that did not have microbial gas generation in the 2004 CRA PA. The points below the line represent the effect of the changes in microbial gas generation rates. At higher pressure, the pressures in the new-rate analysis tend to converge with 2004 CRA PA results as the degradation of organic material becomes more complete.

Figure 10 and Figure 11 show plots for maximum, minimum, and average pressures as a function of time. Although pressure trends in individual vectors are significantly changed from the 2004 CRA PA in the undisturbed scenario, S1, the statistics for pressure are very similar (Figure 10). At short times the pressure in the new-rate analysis is significantly different from the 2004 CRA PA. At sufficiently long times the range of pressures is slightly reduced for S1. The range and average pressure in scenario S2 is very close to the 2004 CRA PA (Figure 11).

The changes implemented in this analysis do not significantly alter the range of pressures or average pressure of 100 vectors in either scenario. It should be noted that the new microbial gas generation rates generally spread the increase in pressure out over a longer period of time, but the maximum pressure in many vectors is similar to the 2004 CRA PA.

S1, Pressure in the Waste Panel New Microbial Gas Generation Rates vs CRA

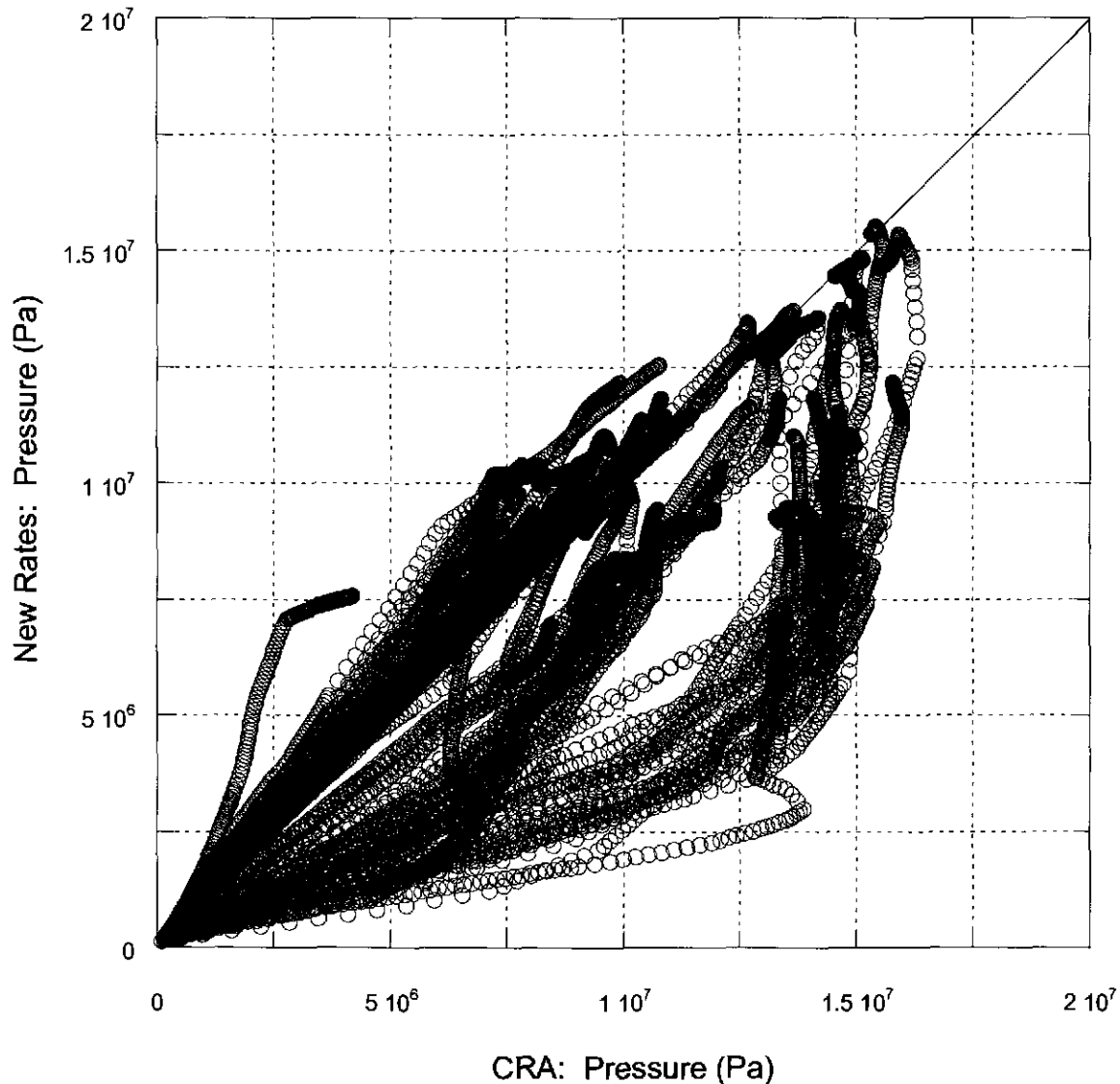


Figure 8. Scatter plot of pressure in the waste panel for scenario S1. Points are pressures in each vector resulting from changes to the gas-generation model described in §4.2 versus results obtained from 2004 CRA PA calculations. The times plotted are listed in Table 3.

S2, Pressure in the Waste Panel
New Microbial Gas Generation Rates vs CRA

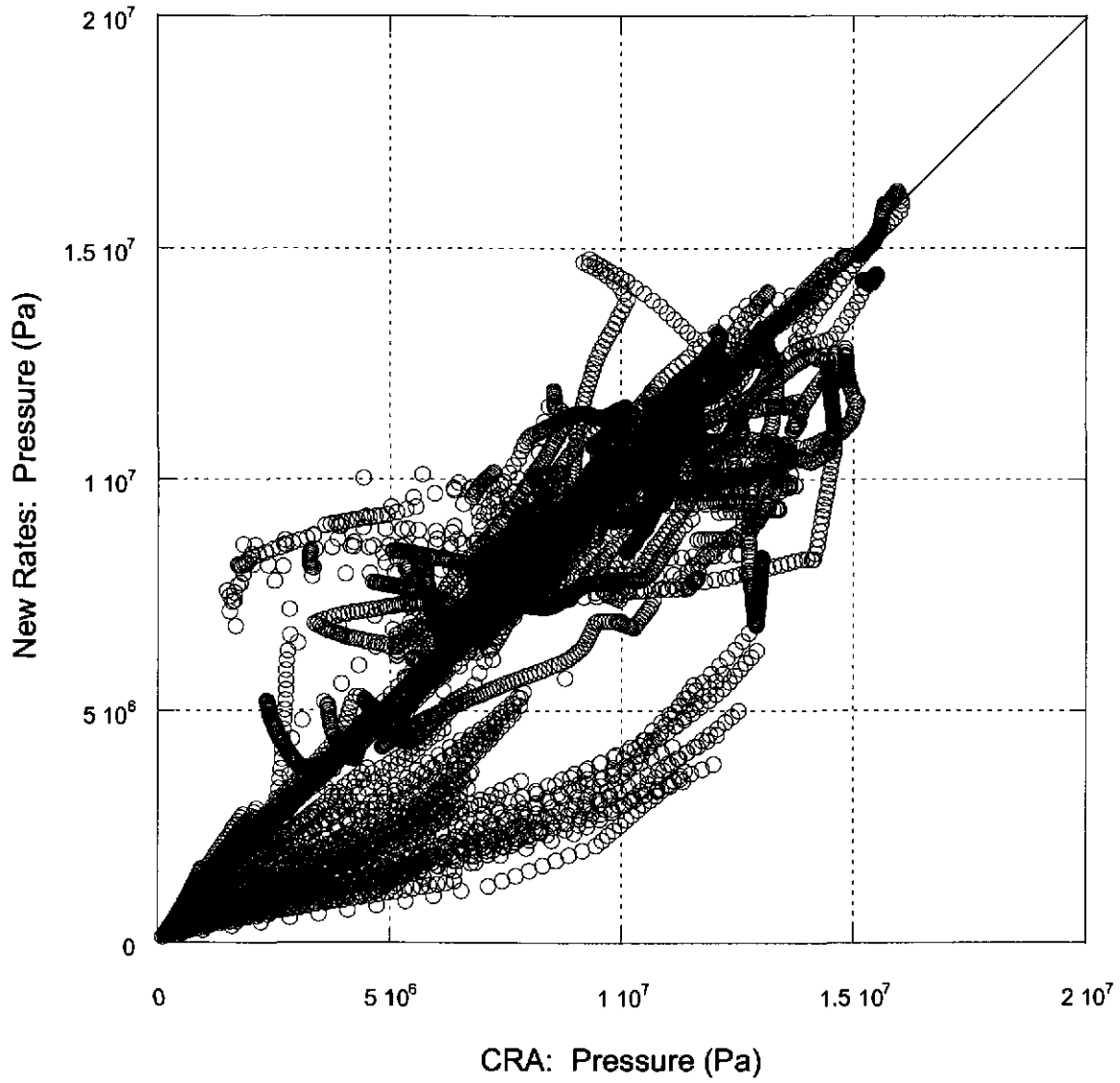


Figure 9. Scatter plot of pressure in the waste panel for scenario S2. Points have the same meaning as in Figure 8.

S1, Statistics for Pressure in the Waste Panel
 New Microbial Gas Generation Rates vs CRA

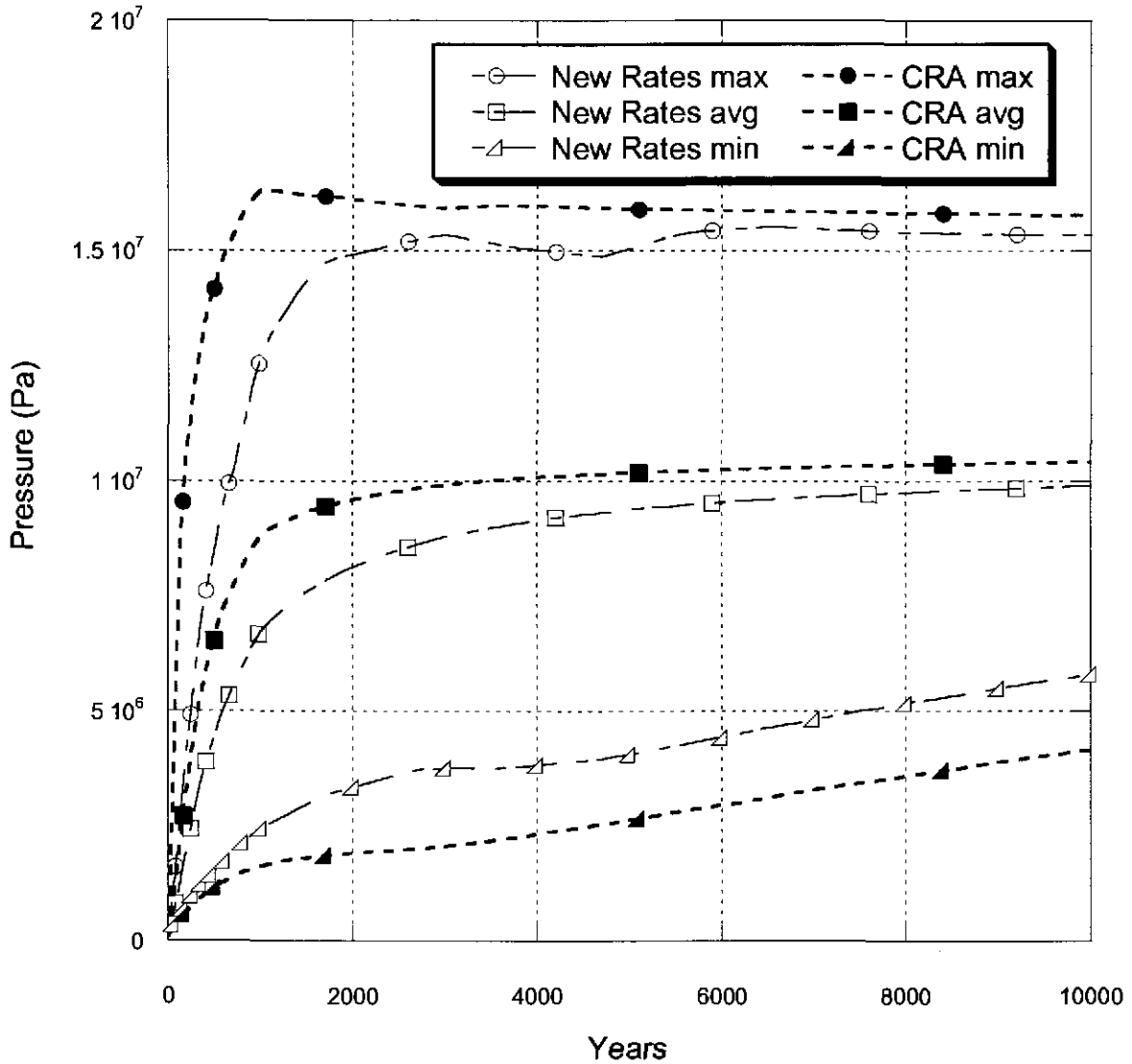


Figure 10. Pressure in the waste panel versus time for scenario S1. Open shape points and corresponding dashed lines represent results with the changes to the gas-generation model described in §4.2. Filled shape points and short dashed lines represent results from the 2004 CRA PA. The maximum pressure curve is the maximum over all vectors at each time plotted, same for the average and the minimum. The times plotted are listed in Table 3.

S2, Statistics for Pressure in the Waste Panel
 New Microbial Gas Generation Rates vs CRA

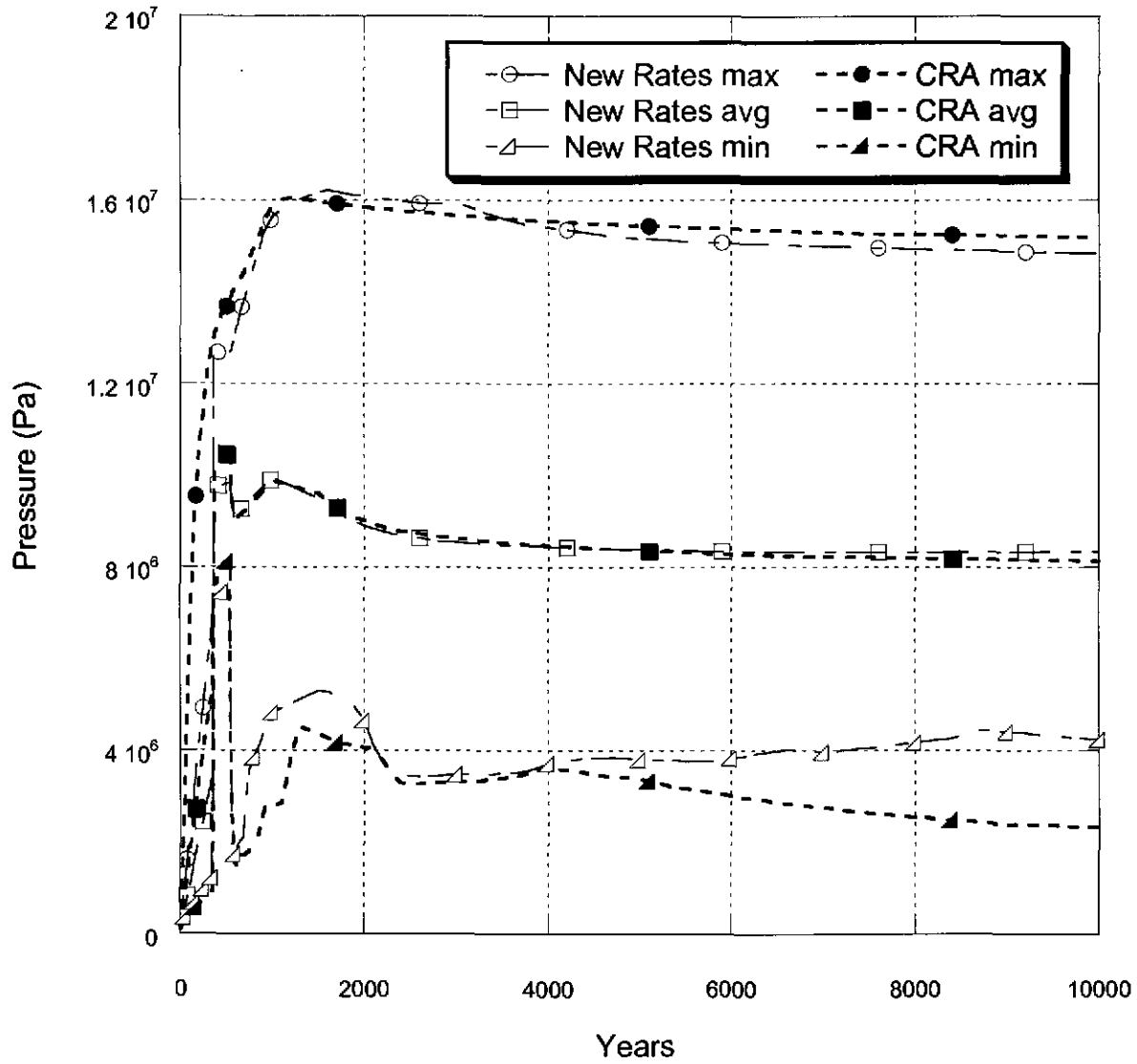


Figure 11. Pressure in the waste panel versus time for scenario S2. Points and lines have the same meaning as in Figure 10.

5.2 *Brine Saturation*

Brine saturation is an input parameter from BRAGFLO into the DBR analysis. DBR releases are dependent upon both pressure and brine saturation. Pressure has to exceed the hydrostatic pressure and brine saturation must exceed the residual brine saturation of waste in order for there to be the possibility of a DBR release during a drilling intrusion.

Brine saturation, especially in individual vectors, is affected by the changes to BRAGFLO modeling simulations (Figure 12 and Figure 13); the changes tend to have a canceling effect on the mean. In the undisturbed scenario, S1, brine saturation tends to be lower in vectors that had no microbial gas generation in the 2004 CRA PA, because increased pressure due to microbial gas generation in the new-rate calculations offers more resistance to brine inflow (Figure 12). The new microbial gas generation rates are lower in the new-rate analysis, which results in a slower increase in pressure (Section 5.1). The slower increase in pressure results in higher brine saturation in many vectors, because the lower pressure presents less resistance to brine inflow.

There is a pronounced increase in brine saturation in many vectors of scenario S2, which includes a drilling intrusion into a pressurized brine pocket in the Castile at 350 years. The slower increase in pressure due to the new microbial-gas-generation rates permits greater inflow of brine from the Castile into the repository. However this does not equate to greater flow of brine up the borehole to the Culebra, as shown in Figure 21.

Figure 14 and Figure 15 present plots of minimum, maximum, and average brine saturation over time for each scenario. The most significant statistic for brine saturation in the waste panel is that the average brine saturation in S2 is about 10% higher in the new-rate calculations versus that of the 2004 CRA PA (Figure 15). The maximum brine saturation in the undisturbed scenario is slightly lower in the new-rate calculations compared to the 2004 CRA PA. Brine inflow and hence brine saturation can be very sensitive to small differences in pressure.

S1, Brine Saturation in the Waste Panel
New Microbial Gas Generation Rates vs CRA

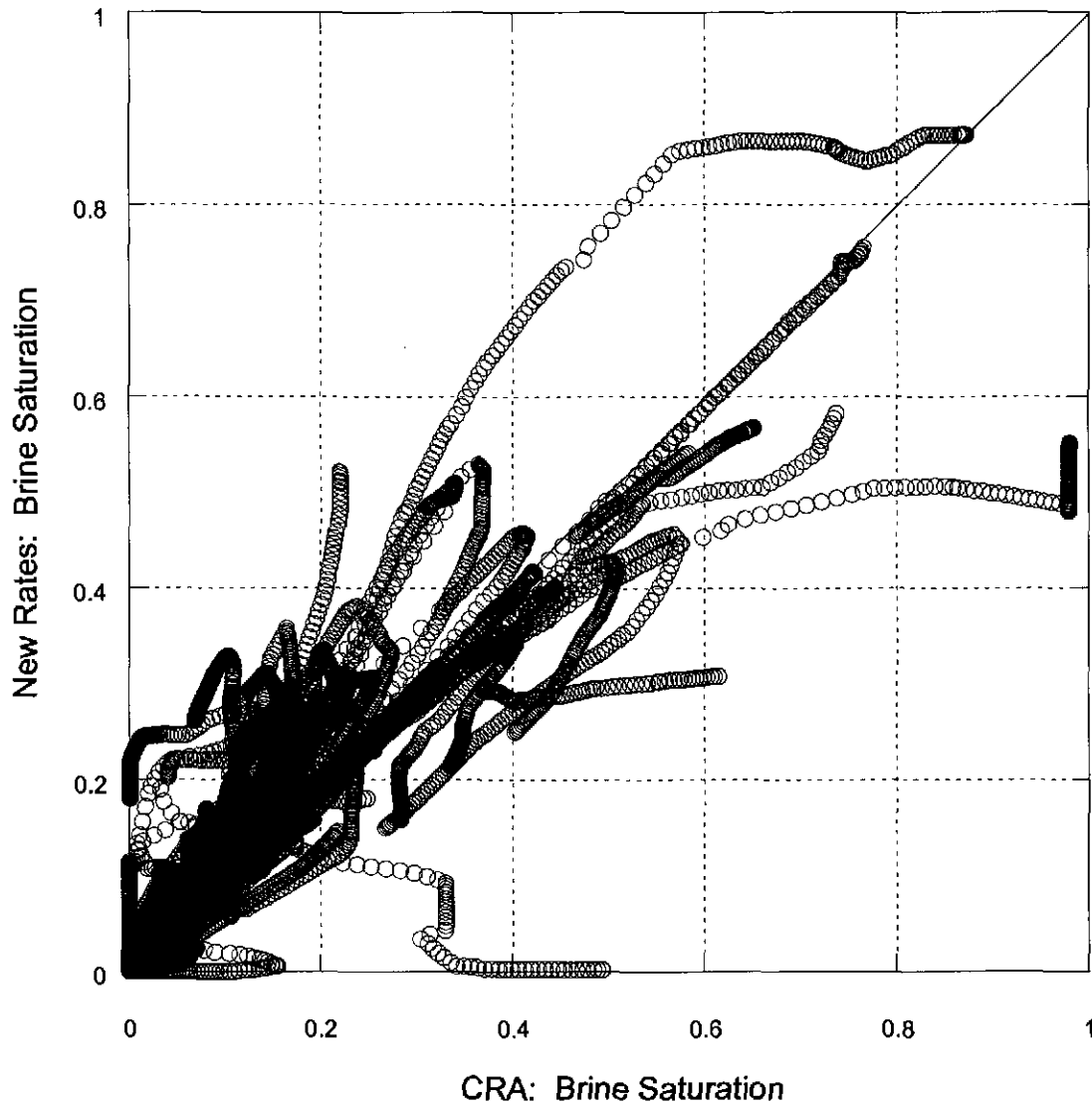


Figure 12. Scatter plot of brine saturation in the waste panel for scenario S1. Points are brine saturations in each vector resulting from changes to the gas-generation model described in §4.2 versus results obtained from 2004 CRA PA calculations. The times plotted are listed in Table 3.

S2, Brine Saturation in the Waste Panel
New Microbial Gas Generation Rates vs CRA

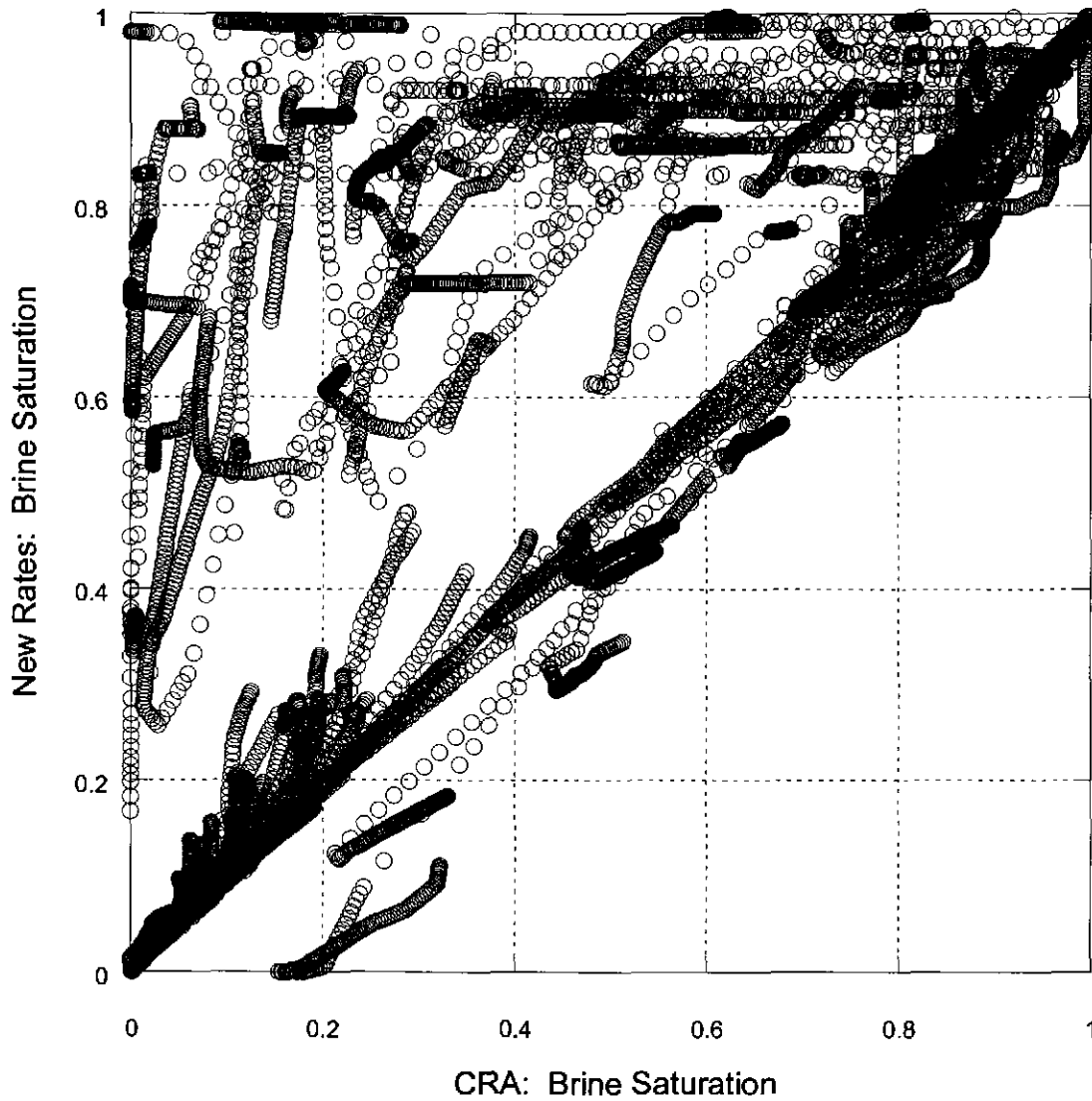


Figure 13. Scatter plot of brine saturation in the waste panel for scenario S2. Points have the same meaning as in Figure 12.

S1, Statistics for Brine Saturation in the Waste Panel
 New Microbial Gas Generation Rates vs CRA

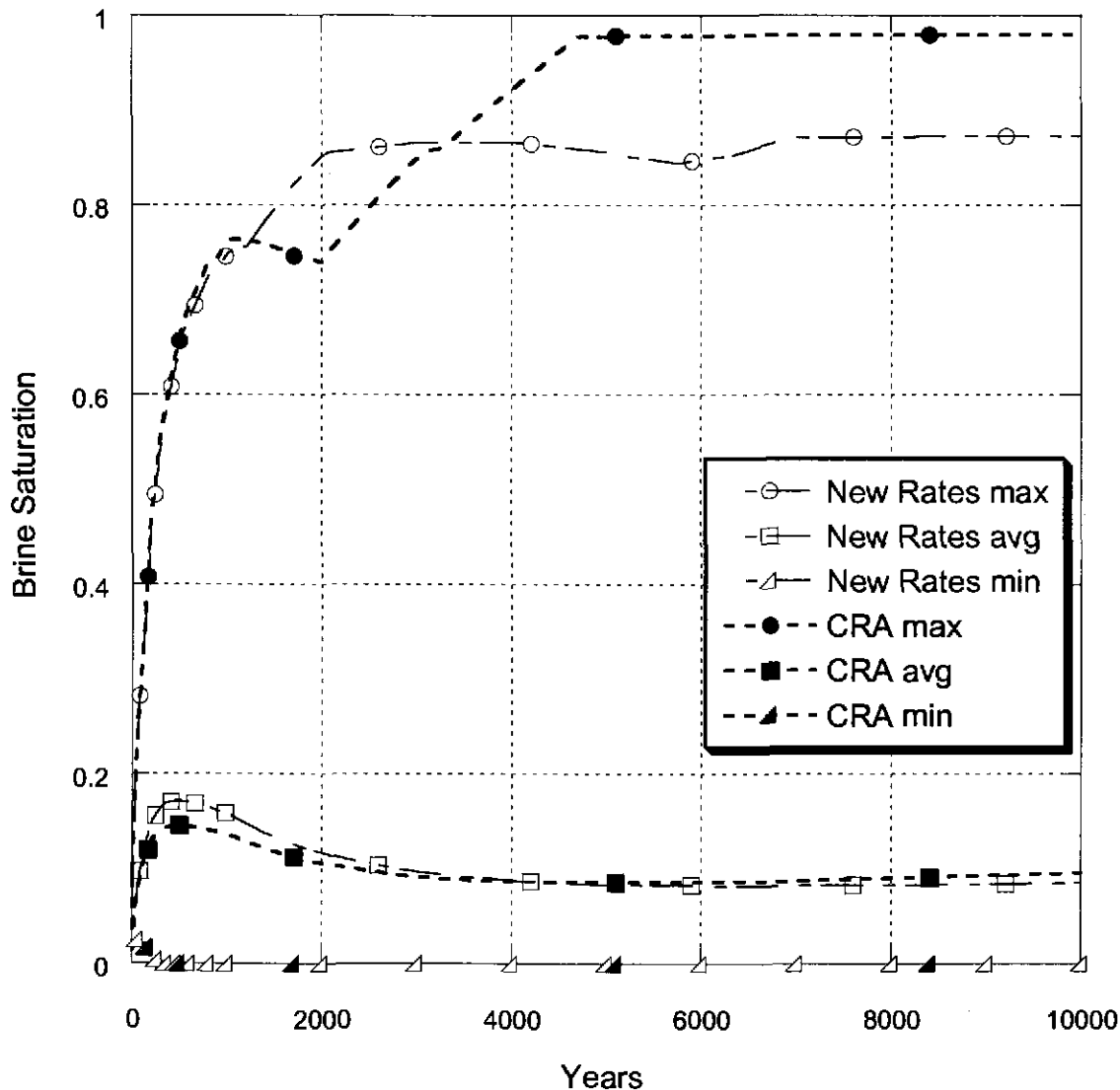


Figure 14. Brine saturation in the waste panel versus time for scenario S1. Open shape points and corresponding dashed lines represent results with the changes to the gas-generation model described in §4.2. Filled shape points and short dashed lines represent results from the 2004 CRA PA. The maximum brine saturation curve is the maximum over all vectors at each time plotted, same for the average and the minimum. The times plotted are listed in Table 3.

S2, Statistics for Brine Saturation in the Waste Panel
 New Microbial Gas Generation Rates vs CRA

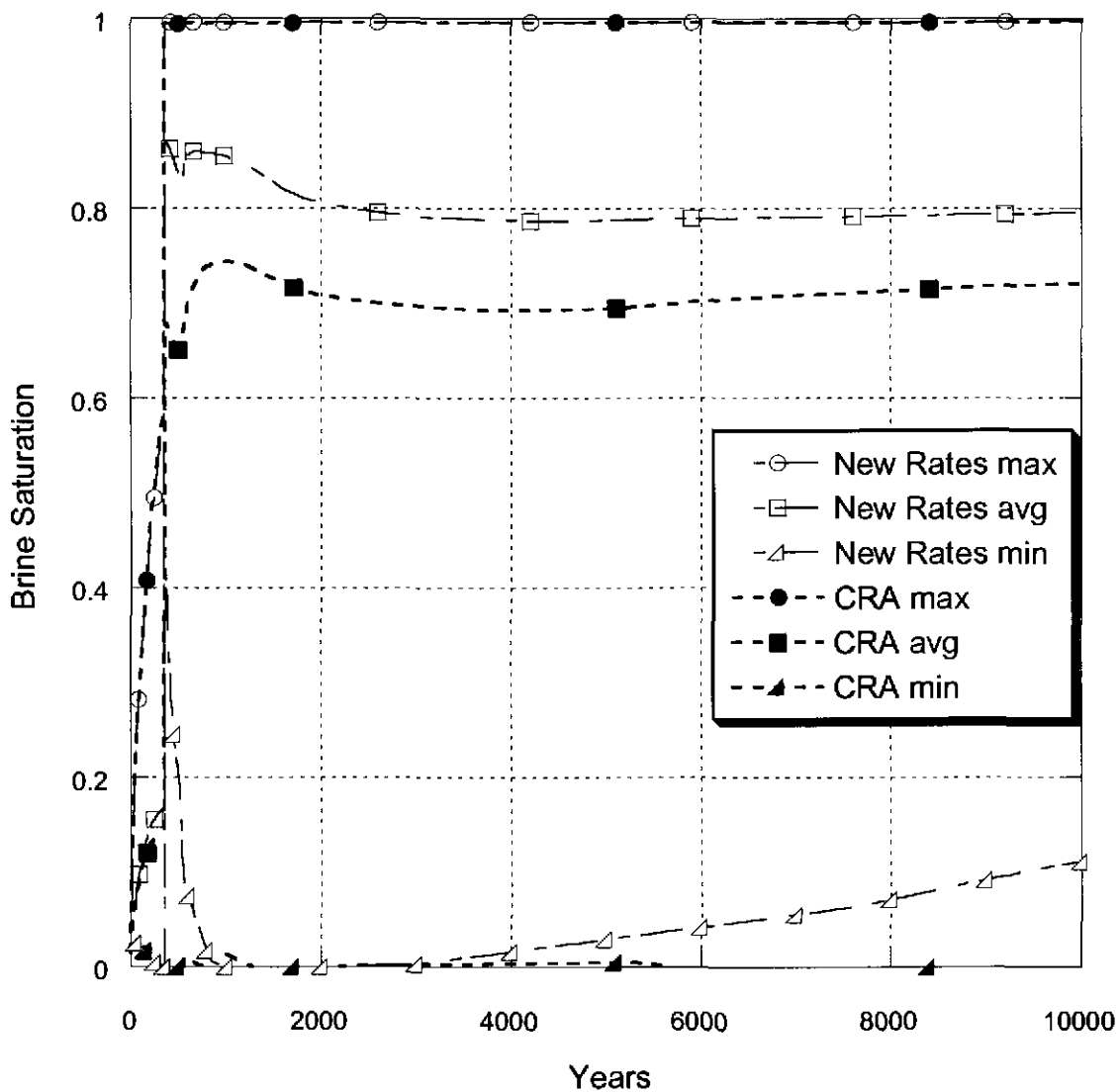


Figure 15. Brine saturation in the waste panel versus time for scenario S2. Points, lines, and colors have the same meaning as in Figure 14.

5.3 Brine Outflow

The primary objective of WIPP PA is to evaluate the potential for radionuclides reaching the surface or the land withdrawal boundaries (LWB). There are two potential pathways for the release of brine containing radionuclides: 1) migration of radionuclides with brine flow along anhydrite marker beds, which are in close proximity to the excavations to the LWB, and 2) migration of contaminated brine up a borehole in drilling-intrusion scenarios to the Culebra and then along the Culebra to the LWB. Total cumulative brine outflow in this analysis includes both types of brine flow away from the repository (into the marker beds and up the borehole). Any significant changes in total cumulative brine outflow (e.g. a pronounced increase in the maximum outflow in a scenario) would indicate that more detailed analysis of specific flows is needed. Follow-up could include flow along specific marker beds, flow up the borehole to the Culebra, or flow along the Culebra, which is analyzed in a subsequent PA step. In the absence of a significant increase in brine outflow, these detailed analyses are not needed.

Previous analyses have consistently shown drilling intrusions to be the most probable pathway for a radionuclide contaminated brine release. Scenario S2, with a drilling intrusion through the repository into a pressurized brine pocket in the Castile Formation, produced the highest brine outflow in the 2004 CRA PA, which is why it was selected for this analysis. The PA application Panel uses brine outflow up the borehole calculated by BRAGFLO as input into an evaluation of potential releases by groundwater flow and transport to the LWB along the Culebra Member of the Rustler Formation bed. The Culebra is the lowest stratigraphic unit above the repository with sufficient transmissivity to potentially transport radionuclides.

Figure 16 and Figure 17 present scatter plots of new-rate brine outflow versus 2004 CRA PA results. Only two vectors in scenario S1 depart from the diagonal line, which represents equal values in both analyses. Vector 22, which had almost 20,000 m³ of brine outflow in the 2004 CRA PA had only about 5,000 m³ in the new-rate analysis (Figure 18). This vector is particularly affected by the new microbial gas generation rates, because it had both a high inundated gas generation rate in the 2004 CRA PA and a high wicking factor. Thus by equation (13) vector 22 had a high gas generation rate in the 2004 CRA PA. All CPR was biodegraded within 200 years, resulting in a corresponding rapid increase in pressure, which released brine from the DRZ by fracturing. Vector 22 also has the second highest halite porosity, which means there was a relatively large amount of brine in the DRZ. The more rapid pressure increase in the CRA simulation caused a greater increase in permeability of the DRZ, compared to this analysis. Consequently, more brine (~15,000 m³) was released into the repository in the CRA simulation. In scenario S2 brine outflow is virtually the same in new-rate and 2004 CRA PA simulations. Brine outflow is slightly higher in the new-rate calculations because lower pressure favors higher brine inflow and brine saturation. However, brine outflow is so dominated by borehole conditions (e.g. the permeability of borehole fill material) that the differences due to microbial gas generation rates are negligible. Plots of maximum, minimum, and average brine outflow in each scenario (Figure 19 and Figure 20) show no significant difference between new-rate and 2004 CRA PA results except for vector 22 in scenario S1.

**S1, Cumulative Brine Outflow
New Microbial Gas Generation Rates vs CRA**

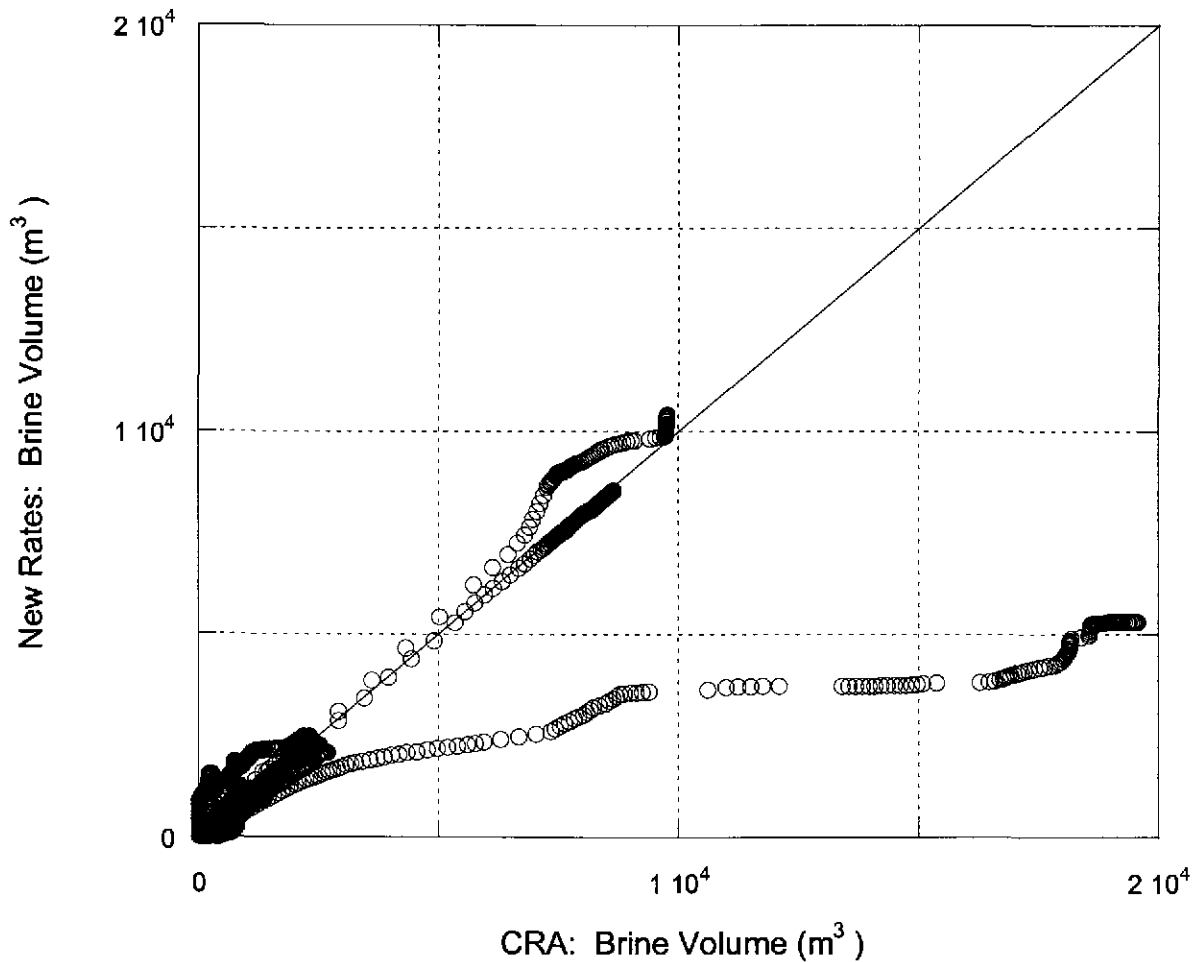


Figure 16. Scatter plot of cumulative brine outflow in the waste panel for scenario S1. Points are brine outflow in each vector resulting from changes to the gas-generation model described in §4.2 versus results obtained from 2004 CRA PA calculations. The times plotted are listed in Table 3.

S2, Cumulative Brine Outflow New Microbial Gas Generation Rates vs CRA

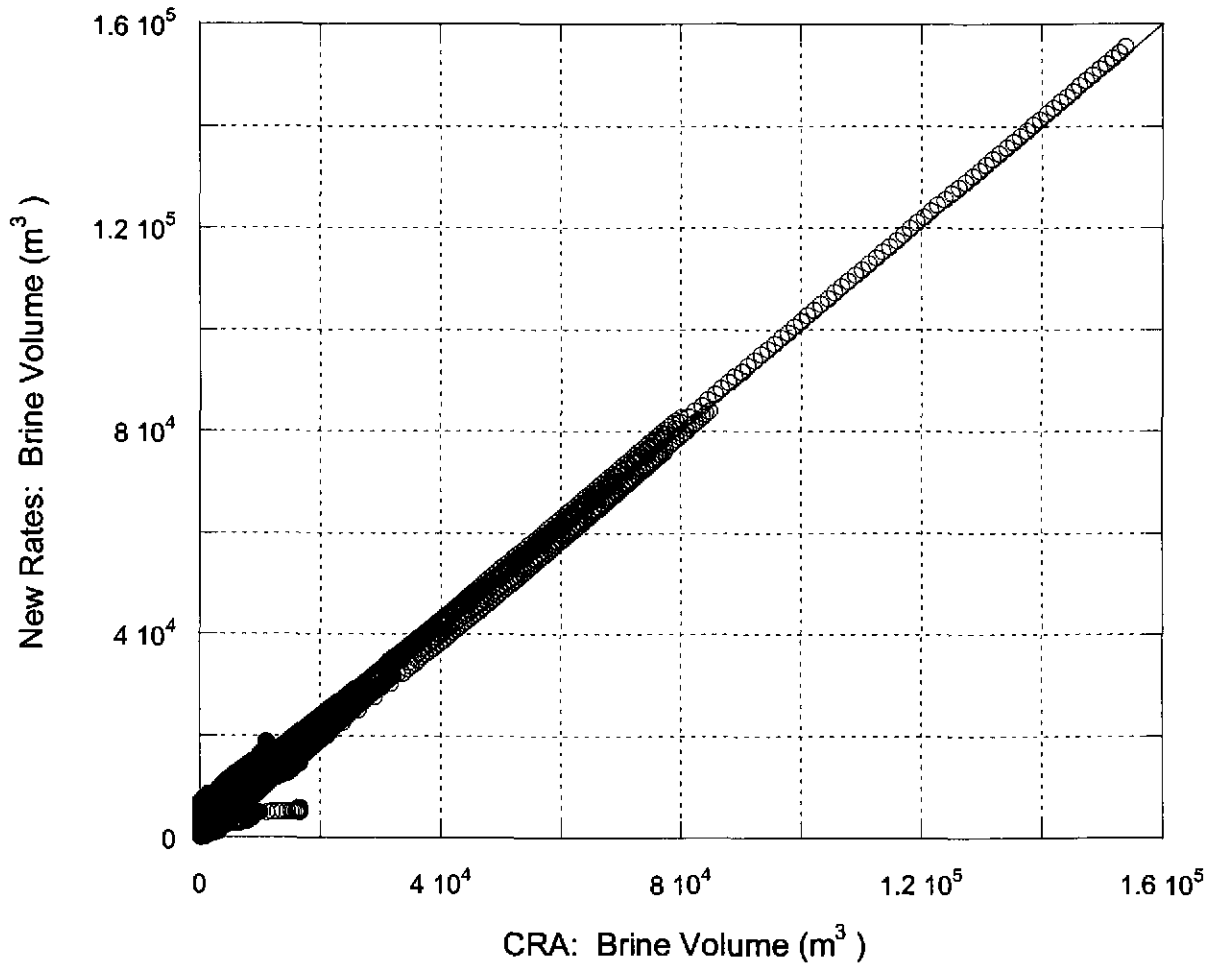


Figure 17. Scatter plot of cumulative brine outflow in the waste panel for scenario S2. Points have the same meaning as in Figure 16.

**S1, Vector 22, Pressure and Brine Flows
New Microbial Gas Generation Rates vs CRA**

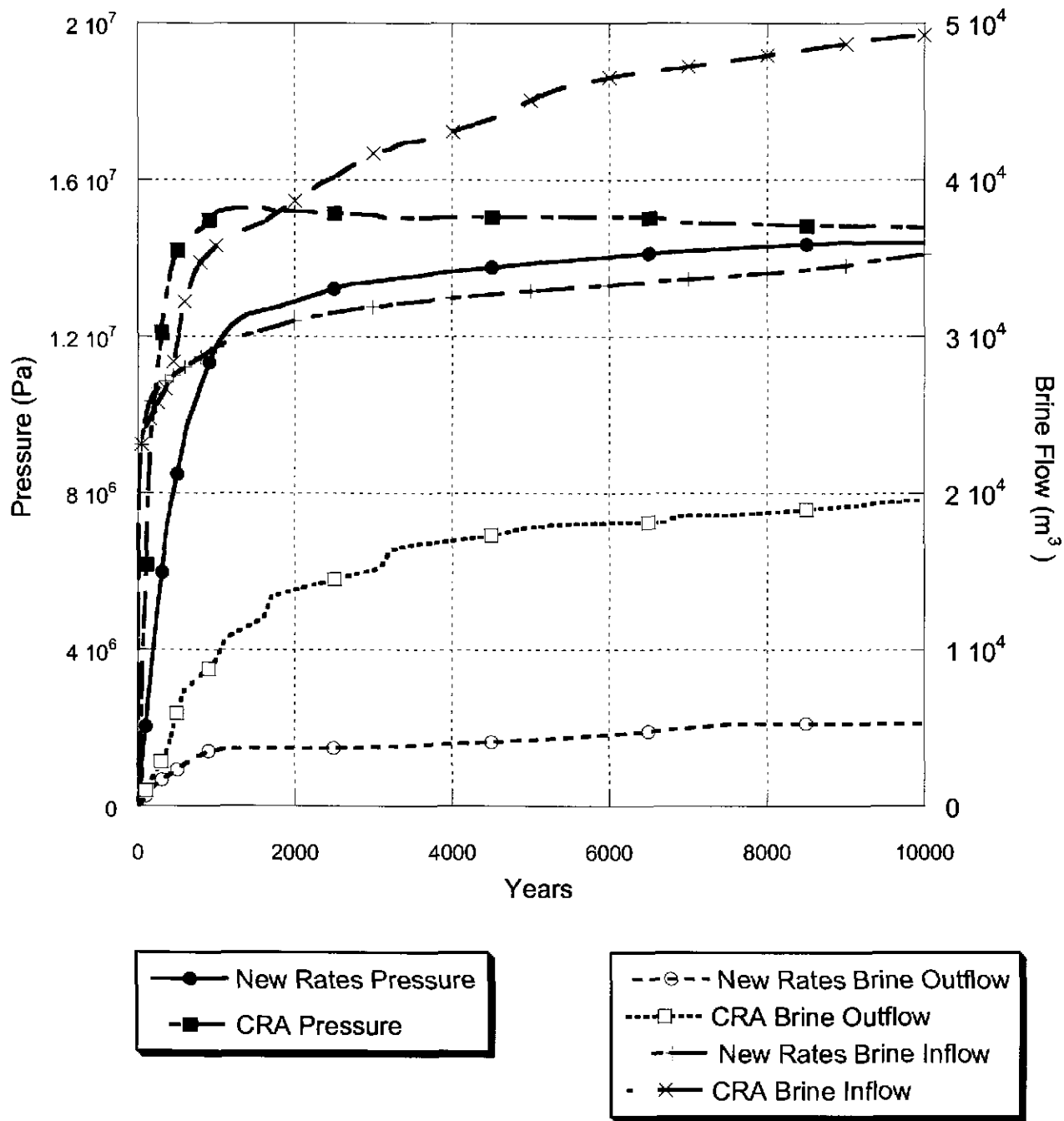


Figure 18. Pressure, cumulative brine inflow and outflow in the waste panel versus time for vector 22 in scenario S1. The times plotted are listed in Table 3. The legend in the above plot defines each curve.

S1, Statistics for Cumulative Brine Outflow New Microbial Gas Generation Rates vs CRA

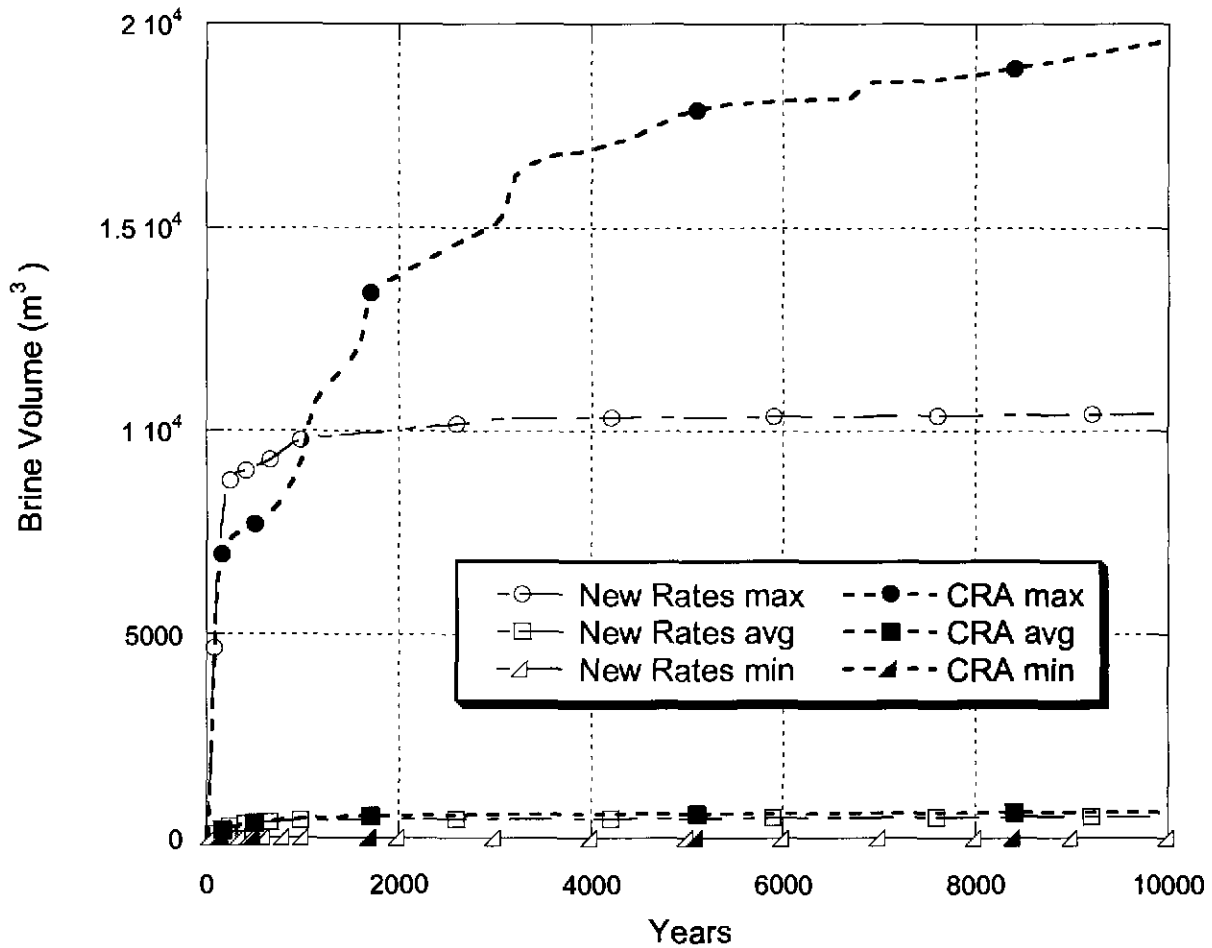


Figure 19. Cumulative brine outflow in the waste panel versus time for scenario S1. Open shape points and corresponding dashed lines represent results with the changes to the gas-generation model described in §4.2. Filled shape points and short dashed lines represent results from the 2004 CRA PA. The maximum brine outflow curve is the maximum over all vectors at each time plotted, same for the average and the minimum. The times plotted are listed in Table 3.

S2, Statistics for Cumulative Brine Outflow New Microbial Gas Generation Rates vs CRA

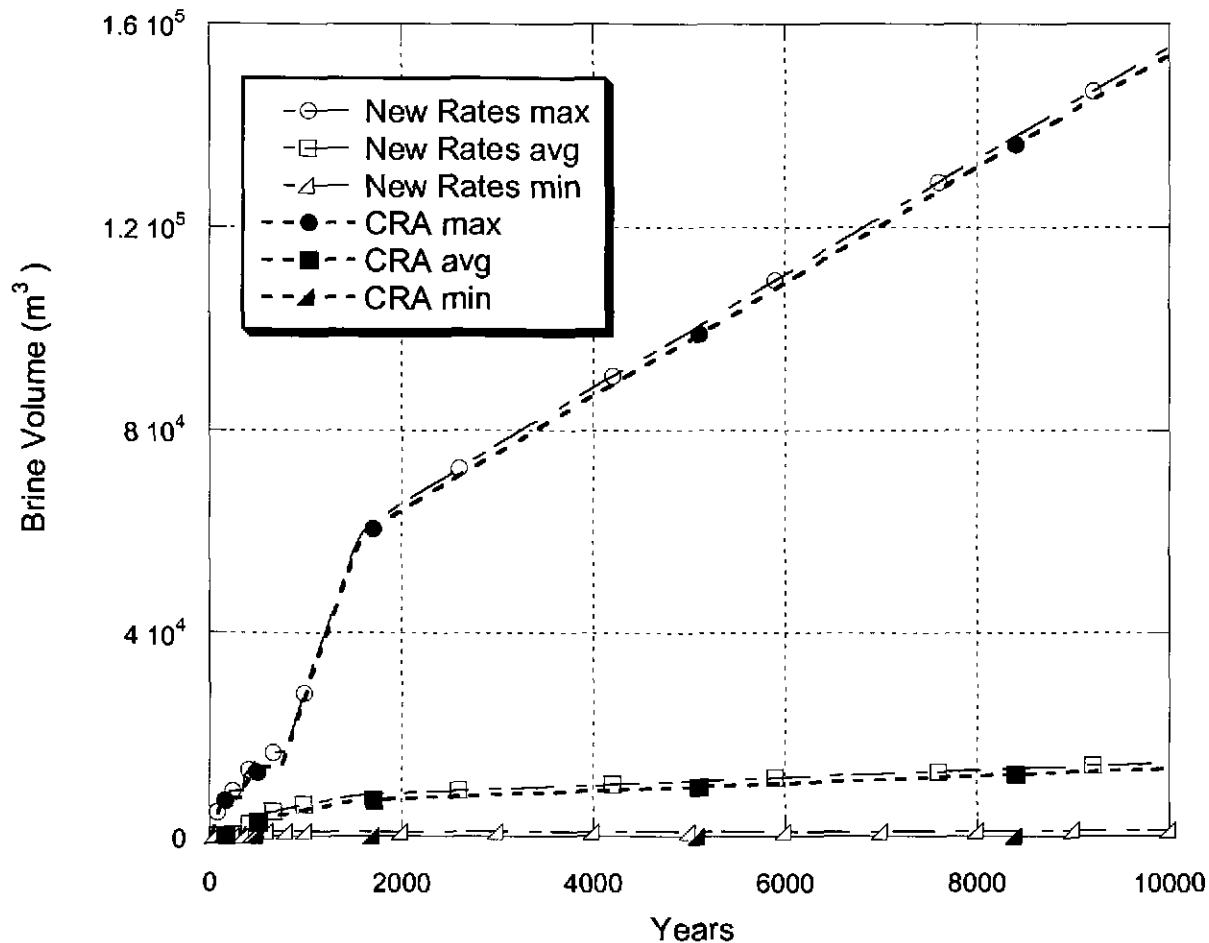


Figure 20. Cumulative brine outflow in the waste panel versus time for scenario S2. Points, lines, and colors have the same meaning as in Figure 19.

Brine Flow Up the Bore Hole At the Base Of The Culebra

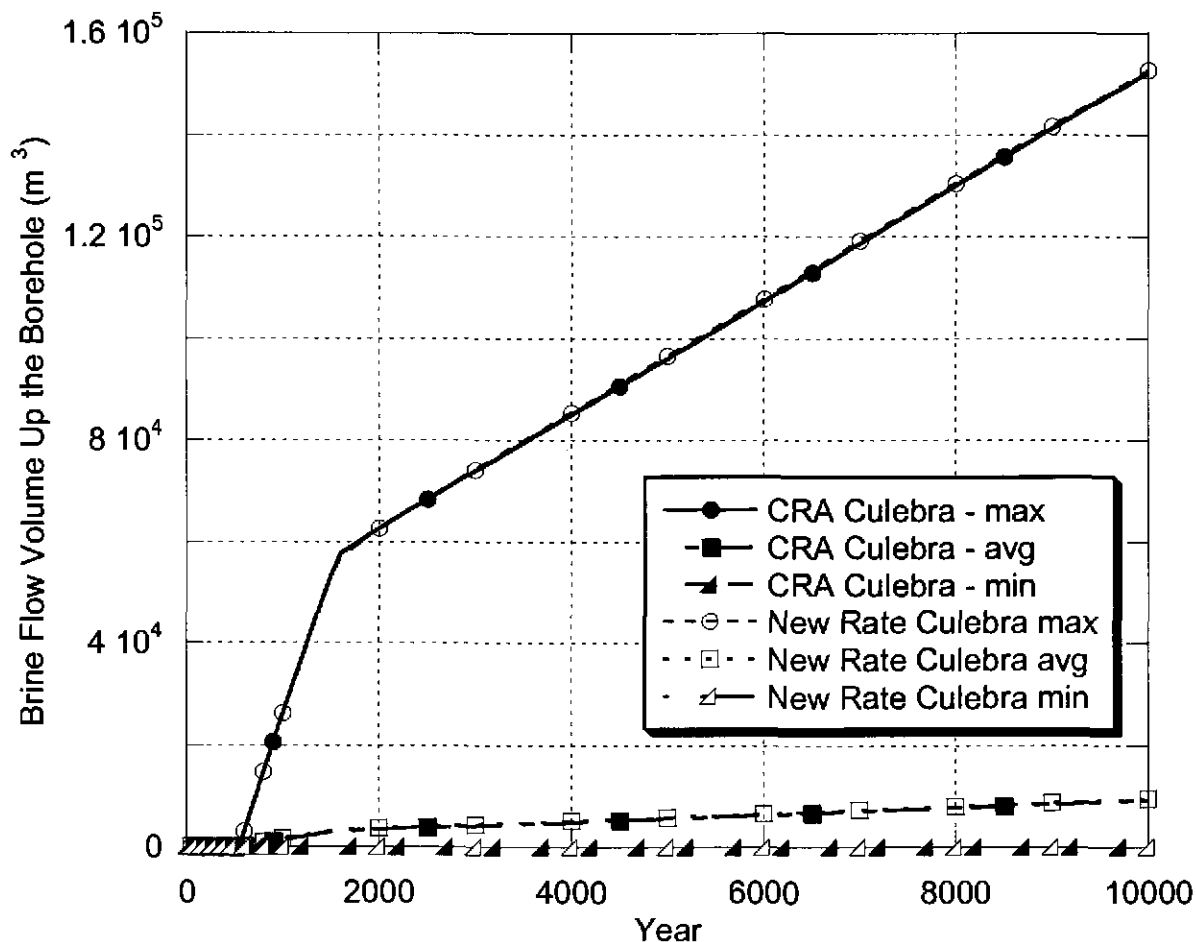


Figure 21. Cumulative brine flow up the bore hole to the Culebra formation. Here solid shapes are the results of the CRA analysis, and open shapes are the results of the new-rate analysis.

6 RUN CONTROL

Digital Command Language (DCL) scripts, referred to here as EVAL run scripts, are used to implement and document the running of all software codes. These scripts, which are the basis for the WIPP PA run control system, are stored in the CRA1_EVAL CMS library. All inputs are fetched at run time by the scripts, and outputs and run logs are automatically stored by the scripts in class CRA1 of the CMS libraries (Table 4-Table 9).

Table 4. BRAGFLO Run Control Files: Step 1

Code	Filename	File Type	CMS LIBRARY, CLASS
BRAGFLO Step 1	<i>run for each replicate. A1 = R1S1 = one run</i>		
Script	EVAL BF CRA1V RUN.COM	script	CRA1V EVAL, MGAS
-	EVAL BF CRA1V RUN MASTER.COM	script	CRA1V EVAL, MGAS
-	EVAL BF CRA1V STEP1.INP	script	CRA1V EVAL, MGAS
-	BF CRA1V MGAS R1 S1 STEP1.LOG	output	CRA1V_BFR1S1, MGAS
-	-	-	-
GENMESH	gm PA96.exe	Executable	wp\$prodroot:[gm.exe]
-	GM BF CRA1V.INP	Input	LIBCRA1V GM, MGAS
-	GM BF CRA1V MGAS.CDB	Output	LIBCRA1V GM, MGAS
-	GM BF CRA1V MGAS.DBG	Output	Temporary (WD)
-	-	-	-
MATSET	matset_qa0910.exe	Executable	wp\$prodroot:[ms.exe]
-	MS BF RATE.INP	Input	LIBCRA1V MS, MGAS
-	GM BF CRA1V MGAS.CDB	Input	LIBCRA1V GM (WD) , MGAS
-	MS BF CRA1V MGAS.CDB	Output	LIBCRA1V MS, MGAS
-	MS MGAS DBG\$OUTPUT.DAT	Output	Temporary (WD)
-	-	-	-
LHS	lhs PA96.exe	Executable	wp\$prodroot:[lhs.exe]
-	LHS1 BF RATE.TRN	Input	LIBCRA1V LHS, MGAS
-	LHS2 BF CRA1V MGAS TRN A1.OUT	Output	LIBCRA1V LHS, MGAS
-	LHS2 BF CRA1V MGAS DBG A1.OUT	Output	LIBCRA1V LHS, MGAS
-	-	-	-
POSTLHS	postlhs PA96.exe	Executable	wp\$prodroot:[lhs.exe]
-	MS BF CRA1V MGAS.CDB	Input	LIBCRA1V MS (WD) , MGAS
-	LHS2 BF CRA1V MGAS TRN A1.OUT	Input	LIBCRA1V LHS (WD) , MGAS
-	LHS3 BF CRA1V.INP	Input	LIBCRA1V LHS , MGAS
-	LHS3 BF CRA1V MGAS A1 R^.CDB	Output	LIBCRA1V LHS, MGAS
-	LHS3 BF CRA1V MGAS A1.DBG	Output	Temporary (WD)
-	LHS3 BF CRA1V MGAS A11.SCR	Output	Temporary (WD)
-	LHS3 BF CRA1V MGAS A12.SCR	Output	Temporary (WD)
-	-	-	-
-	icset PA96.exe	Executable	wp\$prodroot:[ic.exe]

ICSET			
-	LHS3 BF CRA1V MGAS A1 R^.CDB	Input	LIBCRA1V_LHS (WD), MGAS
-	IC BF CRA1V.INP	Input	LIBCRA1V_IC, MGAS
-	IC BF CRA1V MGAS R1 V^.CDB	Output	LIBCRA1V_IC, MGAS
-	IC BF CRA1V MGAS R1 V^.DBG	Output	Temporary (WD)
-	-	-	-
ALGEBRACDB	algebracdb PA96.exe	Executable	wp\$prodroot:[alg.exe]
-	IC BF CRA1V MGAS R1 V^.CDB	Input	LIBCRA1V_IC (WD), MGAS
-	ALG1 BF RATE.INP	Input	LIBCRA1V_ALG, MGAS
-	ALG1 BF CRA1V MGAS R1 V^.CDB	Output	LIBCRA1V_ALG, MGAS
-	ALG1 BF CRA1V MGAS R1 V^.DBG	Output	Temporary (WD)
-	-	-	-

Table 5. BRAGFLO Run Control Files: Step 2

BRAGFLO Step 2		<i>Run for each replicate (R1), scenario (S1-S2), vector (V001-V100) = 200 runs</i>	
Code	Filename	File Type	CMS LIBRARY, CLASS
Script	EVAL BF CRA1V RUN.COM	script	CRA1V EVAL, MGAS
-	EVAL BF CRA1V RUN MASTER.COM	script	CRA1V EVAL, MGAS
-	EVAL BF CRA1V STEP2.INP	script	CRA1V EVAL, MGAS
-	BF CRA1V MGAS R1S%V^STEP2.LOG	output	CRA1V BFR1S%, MGAS
-	-	-	-
PREBRAG	prebrag_qb0700.exe	Executable	wp\$prodroot:[bf.exe]
-	BF1 CRA1V S%.INP	Input	LIBCRA1V_BF, MGAS
-	ALG1 BF CRA1V MGAS R1 V^.CDB	Input	LIBCRA1V_ALG, MGAS
-	BF1 CRA1V MGAS R1 S% V^.DBG	Output	Temporary (WD)
-	BF2 CRA1V MGAS R1 S% V^.INP	Output	LIBCRA1V BFR1S%, MGAS
-	-	-	-

Table 6. BRAGFLO Run Control Files: Step 3

BRAGFLO Step 3	<i>Run for each replicate (R1), scenario (S1-S2), vector (V001-V100) = 200 runs</i>		
Code	Filename	File Type	CMS LIBRARY, CLASS
Script	EVAL BF CRA1V RUN.COM	script	CRA1V EVAL, MGAS
-	EVAL BF CRA1V RUN MASTER.COM	script	CRA1V_EVAL, MGAS
-	EVAL BF CRA1V STEP3.INP	script	CRA1V EVAL, MGAS
-	BF CRA1V MGAS R1S%V^ STEP3.LOG	output	CRA1V BFR1S%, MGAS
-	-	-	-
BRAGFLO	bragflo qa0500.exe	Executable	wp\$prodroot:[bf.exe]
-	BF2 CRA1V MGAS R1 S% V^.INP	Input	LIBCRA1V BFR1S% (WD) , MGAS
-	BF2 CRA1V CLOSURE.DAT	Input	LIBCRA1V BF , MGAS
-	BF2 CRA1V MGAS R1 S% V^.OUT	Output	Temporary (WD)
-	BF2 CRA1V MGAS R1 S% V^.SUM	Output	Temporary (WD)
-	BF2 CRA1V MGAS R1 S% V^.BIN	Output	Temporary (WD)
-	BF2 CRA1V MGAS R1 S% V^.ROT	Output	Temporary (WD)
-	BF2 CRA1V MGAS R1 S% V^.RIN	Output	Temporary (WD)
-	-	-	-
-	-	-	-
POSTBRAG	postbrag PA96.exe	Executable	wp\$prodroot:[bf.exe]
-	BF2 CRA1V MGAS R1 S% V^.BIN	Input	Temporary (WD)
-	ALG1 BF CRA1V MGAS R1 V^.CDB	Input	LIBCRA1V ALG (WD) , MGAS
-	BF3 CRA1V MGAS R1 S% V^.CDB	Output	LIBCRA1V BFR1S% , MGAS
-	BF3 CRA1V MGAS R1 S% V^.DBG	Output	Temporary (WD)
-	-	-	-

Table 7. BRAGFLO Run Control Files: Step 4

BRAGFLO Step 4	<i>Run for each replicate (R1), scenario (S1-S2), vector (V001-V100) = 200 runs</i>		
Code	Filename	File Type	CMS LIBRARY, CLASS
Script	EVAL BF CRA1V RUN.COM	script	CRA1V_EVAL, MGAS
-	EVAL BF CRA1V RUN MASTER.COM	script	CRA1V_EVAL, MGAS
-	EVAL BF CRA1V_STEP4.INP	script	CRA1V_EVAL, MGAS
-	BF CRA1V MGAS R1S%V^_STEP4.LOG	output	CRA1V_BFR1S%, MGAS
-	-	-	-
ALGEBRACDB_2 (POSTALG)	algebracdb PA96.exe	Executable	wp\$prodroot:[alg.exe]
-	BF3 CRA1V MGAS R1 S% V^.CDB	Input	LIBCRA1V_BFR1S% (WD), MGAS
-	ALG2 BF RATE.INP	Input	LIBCRA1V_ALG, MGAS
-	ALG2 CRA1V MGAS R1 S% V^.CDB	Output	LIBCRA1V_BFR1S%, MGAS
-	ALG2 MGAS BF CRA1V R1S%V^.DBG	Output	Temporary (WD)

Table 8. BRAGFLO Run Control Files: Step 3, Exception Runs

BRAGFLO Step 3 Mod	Exception Runs: R1S1V018, R1S2V018, R1S2V098		
Code	Filename	File Type	CMS LIBRARY, CLASS
Script	EVAL BF CRA1V RUN.COM	script	CRA1V EVAL, MGAS
-	EVAL BF CRA1V RUN MASTER.COM	script	CRA1V EVAL, MGAS
-	EVAL BF CRA1V STEP3 MOD.INP	script	CRA1V EVAL, MGAS
-	BF CRA1V MGAS R1S%V^ STEP3.LOG	output	CRA1V BFR1S%, MGAS
-	-	-	-
BRAGFLO	bragflo qa0500.exe	Executable	wp\$prodroot:[bf.exe]
-	BF2 CRA1V MGAS R1 S% V^ MOD.INP	Input	LIBCRA1V BFR1S%, MGAS
-	BF2 CRA1V CLOSURE.DAT	Input	LIBCRA1V BF, MGAS
-	BF2 CRA1V MGAS R1 S% V^ MOD.OUT	Output	Temporary (WD)
-	BF2 CRA1V MGAS R1 S% V^ MOD.SUM	Output	Temporary (WD)
-	BF2 CRA1V MGAS R1 S% V^ MOD.BIN	Output	Temporary (WD)
-	BF2 CRA1V MGAS R1 S% V^ MOD.ROT	Output	Temporary (WD)
-	BF2 CRA1V MGAS R1 S% V^ MOD.RIN	Output	Temporary (WD)
-	-	-	-
-	-	-	-
POSTBRAG	postbrag PA96.exe	Executable	wp\$prodroot:[bf.exe]
-	BF2 CRA1V MGAS R1 S% V^ MOD.BIN	Input	WORKING DIR
-	ALG1 BF CRA1V MGAS R1 V^.CDB	Input	LIBCRA1V ALG (WD), MGAS
-	BF3 CRA1V MGAS R1 S% V^ MOD.CDB	Output	LIBCRA1V BFR1S%, MGAS
-	BF3 CRA1V MGAS R1 S% V^ MOD.DBG	Output	Temporary (WD)

Table 9. BRAGFLO Run Control Files: Step 4, Exception Runs

BRAGFLO Step 4 Mod	Exception Runs: R1S1V098, R1S2V079, R1S2V098		
Code	Filename	File Type	CMS LIBRARY, CLASS
Script	EVAL BF CRA1V RUN.COM	script	CRA1V EVAL, MGAS
-	EVAL BF CRA1V RUN MASTER.COM	script	CRA1V EVAL, MGAS
-	EVAL BF CRA1V STEP4 MOD.INP	script	CRA1V EVAL, MGAS
-	BF CRA1V MGAS R1S%V^ STEP4.LOG	output	CRA1V BFR1S%, MGAS
-	-	-	-
ALGEBRACDB_2 (POSTALG)	algebracdb PA96.exe	Executable	wp\$prodroot:[alg.exe]
-	BF3 CRA1V MGAS R1 S% V^ MOD.CDB	Input	LIBCRA1V BFR1S% (AD), MGAS
-	ALG2 BF RATE.INP	Input	LIBCRA1V ALG, MGAS
-	ALG2 CRA1V MGAS R1 S% V^ .CDB	Output	LIBCRA1V BFR1S%, MGAS
-	ALG2 MGAS BF CRA1V R1S%V^ .DBG	Output	Temporary (WD)

6.1.1 Explanation of Run Control Tables

The preceding tables constitute the run control documentation for the microbial gas calculations. Each table is labeled with the main code, and process step (if applicable). Many code sets are broken down into a first step (step 1) which runs utility codes such as Genmesh (GM), Matset (MS), LHS, etc., and subsequent steps (step 2, ...) which run the primary code along with any pre and post processors. Step 1 codes are generally run once, or once per replicate, while step 2 codes are generally run once per vector.

Run control tables are intended to provide all the information required to document a calculation. The tables contain five columns:

Code — the descriptive common code name (ICSET, ALGEBRACDB, BRAGFLO, etc.) indicating the row relates to that code, “Script” indicating the row relates to the run control system, or blank indicating the row relates to the previous code label. Completely blank rows are for visual separation only.

Filename — VMS filename in the form <filename>.<extension>. Placeholders are included when multiple replicates, scenarios, vectors, ... are being represented (see footnote below).

File Type — the type of file being identified from the point of view of the current step of the run control system. These include script, executable, input, output, and scratch. Note that the output of one step may become the input of an ensuing step.

CMS LIBRARY, CLASS — the CMS library and class where the controlled version of the file can be found, “temporary (wd)” indicating the file is not stored in CMS (many files generated by a calculation are for debug purposes, or are intermediate in nature, and are not retained after execution), “(wd)” or “(ad)” following a CMS library name indicating the input, though stored in CMS, is pulled from the temporary working directory or analysis directory (respectively) for convenience, “working_dir” indicating the input is from a temporary file produced by an earlier code, or other lowercase strings indicating the VMS directory pathname where the file (generally an executable) is located.

-
- R#—used to denote multiple replicates, where # = 1. Seen as Ax in LHS
 - S%—used to denote multiple scenarios, where % = 1-2
 - V^—used to denote multiple vectors, where ^ = 1-100. Seen as R^ in LHS
 - (wd)—working_dir
 - (ad)—analysis_dir

7 REFERENCES

- Berner, R. A. (1980). Early Diagenesis: A Theoretical Approach, Princeton, NJ, Princeton University Press.
- Box, G. E. P., W. G. Hunter and J. S. Hunter (1978). Statistics For Experimenters An Introduction to Design, Data Analysis, and Model Building, New York, John Wiley & Sons.
- Brush, L. H. (2004). Implications of New (Post-CCA) Information for The Probability of Significant Microbial Activity In the WIPP. Sandia National Laboratory, Albuquerque, NM. ERMS #536205.
- Chapelle, F. H. (1993). Ground-Water Microbiology and Geochemistry, New York, NY, John Wiley and Sons.
- Criddle, C. S., L. A. Alvarez and P. L. McCarty (1991). Microbial Processes in Porous Media. Transport Processes in Porous Media. J. Bear and M. Y. Corapcioglu. Amsterdam, Netherlands, Kluwer Academic Publishers: 639-691.
- Fenchel, T., G. M. King and T. H. Blackburn (2000). Bacterial Biogeochemistry: The Ecophysiology of Mineral Cycling, 2nd Edition. San Diego, CA, Academic Press.
- Francis, A. J., J. B. Gillow and M. R. Giles (1997). Microbial Gas Generation Under Expected Waste Isolation Pilot Plant Repository Conditions. Sandia National Laboratories, Albuquerque, NM. SAND96-2582. ERMS#244883.
- Froelich, P. N., G. P. Klinkhammer, et al. (1979). "Early Oxidation of Organic Matter in Pelagic Sediments of the Eastern Equatorial Atlantic: Suboxic Diagenesis." Geochimica et Cosmochimica Acta **43**: 1075-1090.
- Ginevan, M., E. (2004). Statistical Tools for Environmental Quality Management, Chapman & Hall/CRC: p. 92.
- Hunter, K. S., Y. Wang and P. Van Cappellen (1998). "Kinetic modeling of microbially-driven redox chemistry of subsurface environments: coupling transport, microbial metabolism and geochemistry." Journal of Hydrology **209**: 53-80.
- Long, J. J. (2004). Execution of Performance Assessment for the Compliance Recertification Application (CRA1), Revision 1. Sandia National Laboratories, Carlsbad, NM. ERMS 536616.
- Monod, J. (1949). "The growth of bacterial cultures." Annual Review of Microbiology **3**: 371-394.
- Nemer, M. B. and W. Zelinski (2005). Analysis Report for BRAGFLO Modeling Results with the removal of Methanogenesis from the Microbial-Gas-Generation Model. Sandia National Laboratory, Albuquerque, NM. ERMS #538748.

Schlesinger, W. H. (1997). Biogeochemistry: An Analysis of Global Change. New York, NY, Academic Press.

Stein, J. S. and M. B. Nemer (2005). Analysis Plan for Updating the Microbial Degradation Rates for performance Assessment, AP-116. Sandia National Laboratory, Albuquerque, NM. ERMS #538596.

U. S. Congress (1992). Waste Isolation Pilot Plant Land Withdrawal Act. Public Law 102-579, as amended by Public Law 104-201. September 1996. 104th Congress, Washington D.C.

U. S. DOE (2002). January 31st, 2002 Technical baseline Report: Compliance Monitoring and Repository Investigations, Milestone RI110. U.S. Department of Energy Waste Isolation Pilot Plant, Carlsbad, NM. ERMS #520467.

U.S. DOE (2004). Title 40 CFR Part 191 Compliance Recertification Application for the Waste Isolation Pilot. U.S. Department of Energy Waste Isolation Pilot Plant, Carlsbad Field Office, Carlsbad, NM. DOE/WIPP 2004-3231.

U.S. EPA (1993). 40 CFR 191. Environmental Radiation Protection Standards for Management and Disposal of Spent Nuclear Fuel, High-Level and Transuranic Radioactive Wastes: Final Rule. U.S. Environmental Protection Agency, Washington, DC.

U.S. EPA (1996). 40 CFR 194. Criteria for the Certification and Recertification of the Waste Isolation Pilot Plant's Compliance with the 40 CFR Part 191 Disposal Regulations. U.S. Environmental Protection Agency, Washington, DC.

Wang, Y. and L. Brush (1996a). Estimates of Gas-Generation Parameters for the Long-Term WIPP Performance Assessment. Sandia National Laboratory, Albuquerque, NM. Memorandum to Martin S. Tierney, January 26. ERMS #231943.

Wang, Y. and L. Brush (1996b). Modify the Stoichiometric Factor γ in BRAGFLO to Include the Effect of MgO Added to the WIPP Repository As a Backfill. Sandia National Laboratory, Albuquerque, NM. Memorandum to Martin S. Tierney, February 23. ERMS# 232286.

Wang, Y. and P. Van Cappellen (1996). "A Multicomponent Reactive-Transport Model of Early Diagenesis: Application of Redox Cycling in Coastal Marine Sediments." Geochimica et Cosmochimica Acta **60**: 2993-3014.

Appendix A

Here the fits are determined for Figure 4-Figure 7 from the mean cumulative gas versus time data. An example calculation is presented for the inundated, inoculated, amended, with excess nitrate experiment that is plotted in Figure 1 and Figure 4. The remaining data sets and fits in Figure 5-Figure 7 are tabulated a posteriori. In the below calculations and tables only two digits are significant since only two digits are reported in the experimental data; however 6 digits were calculated to avoid round off errors.

Table 10 gives the raw data for the inundated, inoculated, amended, with excess nitrate experiment plotted in Figure 1 and Figure 4. Table 11 lists the values of the short-term slope and intercept b_s , a_s and the long-term slope and intercept b_l , a_l as determined by equations (2)-(3) from the data in Table 10. From Table 11, S is at a minimum when $m = 13$, which from Table 10 occurs at 481 days with $181 \mu\text{mol CO}_2/\text{g}$ cellulose produced. The long-term slope for this data set was 2.01503×10^{-2} , according to Table 11. Given the long-term fit parameters for $m = 13$, from Table 11, we determine the sample variance from equations (6)-(7), and then the variance and standard deviation in the slope from equations (4), (5) and (8). Performing this calculation yields $\sigma(b_l) = 4.37899 \times 10^{-3}$. The confidence interval is then determined from the student's t test. Given that $m = 13$, the number of data points in the long-term fit is 8 and with two fitting parameters the number of degrees of freedom is 6. Thus $x_\alpha = 2.44691$ from Table 22. Mathematica was used to determine x_α ; the Mathematica file is given in Appendix C. From equation (10) the slope and confidence interval is $2.01503 \times 10^{-2} \pm 1.07215 \times 10^{-2}$. The same procedure is repeated for the remaining data sets in Table 13-Table 21.

A.1 Data and analysis for Figure 4.

Table 10. Amount of CO₂ accumulated versus time for the inundated, inoculated, amended, and with excess nitrate experiment (Francis et al., 1997; U. S. DOE, 2002) shown in Figure 1 and Figure 4.

<i>i</i>	Time (days)	μmol CO ₂ /g cellulose	reported standard error (μmol CO ₂ /g cellulose)
1	0	0.47	0.01
2	45	4.29	0.04
3	69	6.1	3.42
4	104	19.7	6.6
5	132	25.8	6.4
6	164	45.4	8.0
7	200	61.4	8.2
8	228	56.2	13.6
9	264	92.8	8.6
10	297	76.4	8.8
11	356	129.2	13
12	411	162.6	13
13	481	181	8
14	591	190	4
15	733	204	3
16	853	186	9
17	1034	212	2
18	1228	194	4
19	2723	251	5
20	3464	236	42

Table 11. Least-Squares slopes and intercepts as a function of m and the resulting residual sum of squares S from the data in Table 10.

m	a_s	b_s	a_l	b_l	S
3	0.50335	0.082017	81.68378	0.064453	51991.58
4	-1.85992	0.17431	89.54301	0.060414	45016.54
5	-2.84737	0.201705	97.60729	0.056394	38648.69
6	-6.00905	0.268121	106.7614	0.051937	31801.89
7	-8.77592	0.314554	115.6098	0.047739	26448.75
8	-7.58248	0.297261	124.5179	0.043628	21895.11
9	-11.3035	0.343193	136.7878	0.038082	15204.07
10	-9.07511	0.318903	146.3849	0.033848	11956.79
11	-13.1132	0.356108	162.8228	0.026745	4788.444
12	-17.5847	0.392677	173.1218	0.022443	3100.435
13	-18.9939	0.402865	178.7738	0.02015	2677.874
14	-14.803	0.376602	181.4126	0.019115	3123.197
15	-7.0168	0.333893	182.6213	0.018662	5044.005
16	3.722499	0.280398	178.0982	0.020265	10182.16
17	12.59063	0.241416	186.4669	0.017414	14138.56
18	23.84235	0.197246	173.6495	0.021585	22308.34

Table 12. Analysis of variance for the data in Table 10 and Table 11. Here ν is the number of degrees of freedom in the fit.

Data set	m	ν	$S_l(m)$	s^2	\bar{t}	$V(b_l)$	$\sigma(b_l)$	x_a
Table 10	13	6	968.289	161.382	1388.38	1.91755×10^{-5}	4.37899×10^{-3}	2.44691

A.2 Data and Analysis for Figure 5

Table 13. Amount of carbon dioxide versus time produced in experiments that were inundated, inoculated, unamended, without excess nitrate (Francis et al., 1997; U. S. DOE, 2002) shown in Figure 2 and Figure 5.

<i>i</i>	Time (days)	$\mu\text{mol CO}_2/\text{g cellulose}$	reported standard error ($\mu\text{mol CO}_2/\text{g cellulose}$)
1	0	2.11	0.04
2	45	3.41	0.04
3	69	3.34	0.02
4	104	3.01	0.14
5	132	3.97	0.1
6	200	5.47	0.34
7	297	6.14	0.3
8	481	9.68	0.24
9	733	11.8	0.3
10	853	12.8	0.5
11	1034	14	0.5
12	1228	13.9	1
13	2723	24	1.7
14	3464	26.1	2.2

Table 14. Least-Squares slopes and intercepts as a function of *m* and the resulting residual sum of squares *S* from the data in Table 13.

<i>m</i>	a_s	b_s	a_l	b_l	<i>S</i>
3	2.22198	0.019246	4.718883	0.006855	36.30048
4	2.490851	0.008746	5.035995	0.006709	32.7762
5	2.421914	0.010658	5.581966	0.006464	23.98555
6	2.204852	0.014693	6.180661	0.006198	16.81813
7	2.29386	0.013451	6.76326	0.005948	12.03949
8	2.133282	0.015108	7.667394	0.005573	4.689925
9	2.330123	0.013566	7.984452	0.00545	4.738124
10	2.442436	0.012802	8.089893	0.005413	5.311829
11	2.600035	0.011938	8.007026	0.005441	6.882747
12	2.896111	0.010602	7.382287	0.005644	13.36706

Table 15. Analysis of variance for the data in Table 13 and Table 14. Here ν is the number of degrees of freedom in the fit.

Data set	<i>m</i>	ν	$S_l(m)$	s^2	\bar{i}	$V(b_l)$	$\sigma(b_l)$	x_a
Table 13	8	5	3.39068	0.678135	1502.29	8.81911×10^{-8}	2.96970×10^{-4}	2.57058

A.3 Data and analysis for Figure 6

Table 16. Amount of carbon dioxide produced versus time in humid experiment (Francis et al., 1997; U. S. DOE, 2002), as shown in Figure 3 and Figure 6.

i	Time (days)	$\mu\text{mol CO}_2/\text{g cellulose}$	reported standard error ($\mu\text{mol CO}_2/\text{g cellulose}$)
1	6	7.7	0.12
2	100	20	3.8
3	140	28.5	7.1
4	415	72.6	24.4
5	2156	155	36
6	2616	135	28
7	2945	115	20

Table 17. Least-Squares slopes and intercepts as a function of m and the resulting residual sum of squares S from the data in Table 16.

m	a_s	b_s	a_l	b_l	S
3	0	0.203678	45.9591	0.033402	2929.208
4	0	0.179159	73.88312	0.022389	1876.133
5	0	0.076357	264.2224	-0.05024	2296.234

Table 18. Analysis of variance for the data in Table 16 and Table 17. Here ν is the number of degrees of freedom in the fit.

Data set	m	ν	$S_l(m)$	s^2	\bar{t}	$V(b_l)$	$\sigma(b_l)$	x_α
Table 16	4	2	1813.15	906.576	2033	2.38279×10^{-4}	1.54363×10^{-2}	4.30265

A.4 Data and analysis for Figure 7

Table 19. Amount of carbon dioxide produced versus time for the inundated, amended, no excess nitrate experiment (Francis et al., 1997; U. S. DOE, 2002) shown in Figure 7.

<i>i</i>	Time (days)	$\mu\text{mol CO}_2/\text{g cellulose}$	reported standard error ($\mu\text{mol CO}_2/\text{g cellulose}$)
1	0	-0.06	0
2	45	3.79	0.04
3	69	-3.28	0.34
4	104	7.22	0.6
5	132	18.2	1.4
6	164	24.2	0.6
7	200	26	0.8
8	228	26.6	2
9	264	33.6	0.4
10	297	23.2	0.6
11	356	36.2	0.2
12	411	43.2	0.4
13	481	44.4	0.6
14	591	44.4	1
15	733	49.1	0.6
16	853	51.1	0.5
17	1034	52	1
18	1228	49.2	0.8
19	2718	66.9	1.1
20	3464	55.4	2.6

Table 20. Least-Squares slopes and intercepts as a function of m and the resulting residual sum of squares S from the data in Table 19.

m	a_s	b_s	a_l	b_l	S
3	1.278386	-0.02969	25.79318	0.013759	2808.228
4	-0.72219	0.048435	28.74216	0.012242	1847.713
5	-3.38221	0.122232	31.15752	0.011037	1344.137
6	-4.95313	0.155231	32.82289	0.010226	1141.749
7	-4.93444	0.154918	34.12744	0.009606	1023.275
8	-4.26416	0.145205	35.53177	0.008958	917.9834
9	-4.18432	0.14422	37.25268	0.008179	780.7503
10	-1.76422	0.117839	38.2851	0.007723	896.6842
11	-1.11369	0.111845	41.85533	0.00618	550.5562
12	-0.8616	0.109784	43.731	0.005396	478.0621
13	0.233623	0.101866	44.51798	0.005076	505.1526
14	2.543186	0.087392	45.42292	0.004721	653.7513
15	4.923673	0.074335	47.12433	0.004083	814.6271
16	6.939642	0.064293	47.722	0.003871	997.2001
17	9.26584	0.054068	47.65431	0.003894	1279.309
18	11.85369	0.043909	47.11135	0.004071	1717.642

Table 21. Analysis of variance for the data in Table 19 and Table 20. Here ν is the number of degrees of freedom in the fit.

Data set	m	ν	$S_l(m)$	s^2	\bar{t}	$V(b_l)$	$\sigma(b_l)$	x_α
Table 19	12	7	157.455	22.4936	1279.22	2.43155×10^{-6}	1.559343×10^{-3}	2.364624

Table 22. Values of x_α in equation (9) for determining the 95% confidence interval using the student's t distribution . Here ν is the number of degrees of freedom. This table was generated using Mathematica. The Mathematica script is given in Appendix C.

ν	x_α
1	12.706204736174694
2	4.302652729749464
3	3.182446305283708
4	2.7764451051977934
5	2.5705818356363146
6	2.4469118511449690
7	2.3646242515927844
8	2.3060041352041676
9	2.2621571627982044
10	2.2281388519862735

Appendix B

Here the CPR inventory is tabulated and converted to moles of organic carbon. Table 23 lists the various types of CPR materials in the WIPP repository and their total masses. All values were obtained from the WIPP parameter database.

Table 23. Cellulosics inventory from the 2004 CRA PA. The volume of the contact-handled waste and the volume of the remote-handled waste were obtained from WAS_AREA:VOLCHW and WAS_AREA:VOLRHW respectively in the parameter database

Type of cellulose	contact (CH) or remote handled (RH)	WAS_AREA property in the parameter database	Density (kg/m ³)	Volume (m ³)	Total mass (kg)
CELL	CH	DCELLCHW	58	1.68500E+05	9.77300E+06
-	RH	DCELLRHW	4.5	7080	3.18600E+04
-	Total	-	-	-	9.80486E+06
RUB	CH	DRUBBCHW	14	1.68500E+05	2.35900E+06
-	RH	DRUBBRHW	3.1	7080	2.19480E+04
-	Total	-	-	-	2.38095E+06
PLAS	CH	DPLASCHW+DPLSCCHW	58	1.68500E+05	9.77300E+06
-	RH	DPLASRHW+DPLSCRHW	6.3	7080	4.46040E+04
-	Total	-	-	-	9.81760E+06

Given the total masses of the three types of CPR materials, cellulose, rubber and plastic, we can find their equivalent amounts of cellulose using conversion factors (Wang and Brush, 1996a). This is accomplished in Table 24.

Table 24. Conversion of the masses of cellulose, plastics, and rubber into equivalent amounts of cellulose. Conversion factors were obtained from Wang and Brush, 1996a.

Type of material	Mass (kg)	Conversion factor	Converted mass (kg)
cell	9.80486E+06	1	9.80486E+06
rubber	2.38095E+06	1	2.38095E+06
plastics	9.81760E+06	1.7	1.66899E+07
Total	-	-	2.88757E+07

Thus given the total equivalent mass of cellulose 2.88757×10^7 kg, we convert to total moles of organic carbon by

$$\text{mol C} = \text{kg cellulose} \times \frac{1000 \text{ mol cellulose}}{162 \text{ kg cellulose}} \times \frac{6 \text{ mol C}}{\text{mol cellulose}}, \quad (19)$$

where as in equation (15) $162/1000$ is the molecular weight of cellulose in mol/kg and there are 6 mol of organic carbon in 1 mol of cellulose ($C_6H_{10}O_5$). Inserting the total mass 2.88757×10^7 kg into equation (19) yields 1.06947×10^9 mol organic C.



Appendix C: Student's t distribution values of X_α

Below the values of x_α in equation (10) from the student's t distribution are tabulated for 1-10 degrees of freedom using *Mathematica's* Quantile function with the StudentTDistribution[i], where i is the number of degrees of freedom. The Quantile function takes two parameters, the distribution and the desired probability level, which is 0.975 and corresponds to the 95% confidence interval, see Box et al. (1978)

```
<<Statistics`ContinuousDistributions`
```

```
t0 = Table[{i, InputForm[Quantile[StudentTDistribution[i], 1 - 0.05 / 2]]}, {i, 1, 10}];
```

```
MatrixForm[t0]
```

```
( 1  12.706204736174694 )
( 2  4.302652729749464  )
( 3  3.182446305283708  )
( 4  2.7764451051977934 )
( 5  2.5705818356363146 )
( 6  2.446911851144969  )
( 7  2.3646242515927844 )
( 8  2.3060041352041676 )
( 9  2.2621571627982044 )
(10  2.2281388519862735 )
```